POLITECNICO DI TORINO

Department of Mechanical and Aerospace Engineering
Master's Degree in Aerospace Engineering

Master's Thesis

CONCEPTUAL DESIGN METHODOLOGY FOR AN ENVIRONMENTALLY SUSTAINABLE SUPERSONIC AIRCRAFT

MORE&LESS

MDO and REgulations for Low-boom and Environmentally Sustainable Supersonic Aviation

Candidate
Alessandro Galassi

Supervisor
Davide Ferretto

Advisor
Roberta Fusaro
Grazia Piccirillo
Nicole Viola

Academic Year 2022-2023

"May the wind always be at your back,
the sun upon your face,
and the winds of destiny carry you aloft
to dance with the stars."
Blow, 2001

Abstract

The growing need for mass travel in an increasingly connected world and the urgent awareness of climate change are stimulating the search for advanced high-speed aviation solutions.

Supersonic flight symbolises an innovative and extremely attractive subject in the field of aerospace engineering. Initial research was carried out after the Second World War, but it was not until the following decades that real research and development programs, financed by the world powers of the time, took hold. Studies led to the realisation of never-before-seen examples, but the high maintenance, low fuel economy and environmental impact also revealed their many limitations.

In recent times, there has been renewed interest in supersonic flight, thanks to technological updates in aerodynamics, propulsion, structure and control. Specifically, the most urgent challenge is related to increasing pollutant emissions and climate change on our planet. The critical issue has become even more pressing following the approval of the *Green Deal* in 2020, a European plan to make our continent carbon-neutral by 2050, keeping global warming below 2° C compared to pre-industrial levels.

The aim of the thesis was therefore to develop a conceptual design for a sustainable supersonic commercial aircraft, operating in the cruise condition at Mach 2 and powered by biofuel. The fundamental objective consists in examining environmental data in terms of noise and pollutant emissions in the LTO cycle, from the earliest stages of the iterative process, by means of a simplified statistical approach, which surpasses the criteria shown so far in the literature. Thanks to the analytical relationships between the data themselves, numerical results are obtained that can be easily integrated into the Matching Chart, in order to identify, albeit not perfectly accurately, the design point.

Specifically, the project outlined here starts from the following assumptions: cruising Mach equal to 2, number of passengers equal to 100, range of 6000 km and biofuel as propellant. It is articulated through a series of phases: creation of the statistical database, calculation of the initial sizing, definition of the mission profile, description of the aerodynamic model, initialisation of the iterative cycle, elaboration of the Matching Chart, calculation of the updated sizing and investigation of biofuel properties. The methodology makes it possible to determine a design point that meets precise operational and environmental requirements, to estimate the performance and geometric characteristics of the aircraft, and to evaluate the most suitable biological propellant type.

In conclusion, this study offers a guiding tool for engineers and stakeholders in the aeronautical sector, contributing to the realisation of a future in which supersonic transport is not only synonymous with high speed, but also with environmental sustainability.

Contents

Acronyms **1**

Nomenclature **3**

1 Introduction **7**

1.1 Supersonic Flight: Historical Background and Challenges 7

1.2 Conceptual Design 9

1.2.1 Models Proposed in the Literature 10

1.2.2 Model Under Analysis 11

1.3 Regulations 15

2 Statistical Database **17**

2.1 Candidate Family 17

2.2 Performance and Geometric Characteristics 25

3 Initial Sizing **27**

4 Mission Profile **31**

5 Aerodynamic Model **33**

5.1 Lift Coefficient 33

5.2 Drag Coefficient 34

6 Iterative Cycle **37**

6.1 Fuel Mass Fraction 37

6.2 Empty Mass Fraction 38

6.3 Maximum Take Off Mass 38

7 Matching Chart **39**

7.1 Operational Requirements 39

7.2 Environmental Requirements 43

7.3 Design Point 47

8 Updated Sizing **49**

8.1 Profile 51

8.2 Engine 52

8.3 Sonic Boom 52

9 Biofuel **55**

9.1 CO2 Emissions 55

9.2 Costs 59

9.3 Considerations for the Future 60

10 Conclusions **63**

Bibliography **67**

Acronyms

AJF Alternative Jet Fuels

ANOPP Aircraft Noise Prediction Program

AR Aspect Ratio

ASTRID Aircraft on board Systems sizing and TRade off analysis in Initial Design

CAEP Committee for Aviation Environmental Protection

CFD Computational Fluid Dynamics

$\mathbf{EPNL}_A$ Approach Effective Perceived Noise Level

$\mathbf{EPNL}_F$ Flyover Effective Perceived Noise Level

$\mathbf{EPNL}_L$ Lateral Effective Perceived Noise Level

GHG Greenhouse Gas

HSCT High-Speed Commercial Transport

ICAO International Civil Aviation Organisation

ILUC Induced Land Use Change

LCA Life Cycle Assessment

$\mathbf{LIMIT}_A$ Approach Effective Perceived Noise Level Limit

$\mathbf{LIMIT}_F$ Flyover Effective Perceived Noise Level Limit

$\mathbf{LIMIT}_L$ Lateral Effective Perceived Noise Level Limit

LTO Landing Take Off

MAC Mean Aerodynamic Chord

MORELESS MDO and REgulations for Low-boom and Environmentally Sustainable Supersonic aviation

MTOM Maximum Take Off Mass

NASA	National Aeronautics and Space Administration
OEM	Operating Empty Mass
SAF	Sustainable Aviation Fuel
SFC	Specific Fuel Consumption
TOM	Take Off Mass

Nomenclature

α Angle of Incidence

η Airfoil Efficiency

Λ Sweep Angle

λ Taper Ratio

μ Mach Cone Angle

Π Throttle Percentage

π_∞ Reference Pressure Ratio

ρ Density

σ Density Ratio

A Cross-Sectional Area of a Sears–Haack Body

b Span

C_D Drag Coefficient

C_L Lift Coefficient

c_r Root Chord

c_t Tip Chord

$C_{D_{misc}}$ Additional Drag Component

$C_{D_{wv}}$ Extra Drag at Supersonic Speeds

C_{f_c} Skin Friction Coefficient

$C_{L_{max}}$ Maximum Lift Coefficient

CO Carbon Monoxide

CO_2 Carbon Dioxide

E	Aerodynamic Efficiency
e	Oswald Efficiency Factor
F	Fuselage Lift Factor
FF_c	Component Form Factor
g	Gravitational Acceleration
G_{2nd}	Second Segment Climb Gradient
G_{sub}	Subsonic Climb Gradient
G_{sup}	Supersonic Climb Gradient
HC	Unburned Hydrocarbons
k_L	Loftin Parameter
L	Length
l_{land}	Maximum Landing Field Length
l_{TO}	Maximum Take Off Distance
M	Mach Number
N_{eng}	Engine Number
NO_x	Nitrogen Oxides
PM	Particulate Matter
Q_c	Interference Effect Factor
q_∞	Dynamic Pressure
R	Partial Range
R_{max}	Maximum Radius
S	Area
S_{exp}	Wing Reference Area less the Part covered by Fuselage
S_{ref}	Wing Reference Area
S_{wet_c}	Aircraft Wetted Surface
T	Thrust
V	Volume of a Sears–Haack Body

v	Speed
W	Weight
W_{kg}	Mass
x	Distance Ratio

Chapter 1

Introduction

1.1 Supersonic Flight: Historical Background and Challenges

Supersonic flight represents one of the most significant and fascinating challenges in aeronautical and space engineering. The desire to exceed the speed of sound has fascinated mankind for decades and the achievement of this milestone has led to numerous technological advances and changes in aviation history.

The concept of high-speed flight has roots dating back to the second half of the 20th century. Although the first ideas came to life after the Second World War, it was only in the following years that various research and development programs were initialised by the world's major powers, with the aim of investigating the phenomena typical of such a flight regime and developing a design solution capable of reducing mission times and, therefore, the economic impact compared to subsonic aircraft[1].

The first breaking of the sound barrier, by the experimental *Bell X-1* aircraft on 14th October 1947, ushered in the era of supersonic flight, initially in the military with the *Lockheed F-104 Starfighter* and the *Mikoyan-Gurevich MiG-21* aircraft, later in the civil sector with the *Tupolev Tu-144*.

"Military aircraft have been able to pass the so-called *sound barrier* in routine flights since about 1960. A few exceptional types achieved continuous speeds higher than Mach 3 at altitudes above 20 km" [25].

Starting in 1975, the development of a supersonic airliner became a challenge for the aeronautical community, resulting in investments to develop a new generation of HSCT (*High-Speed Commercial Transport*) aircraft. Thus, in 1976 the *Aérospatiale-BAC Concorde* was born, designed for the direct London-New York and Paris-New York routes. It had a slender body and very thin straight wings, similar to contemporary supersonic bombers, and a 120-passenger cabin. The *Concorde* was therefore a top aircraft, offering premium and necessarily high fares: "in the year 2000 the return ticket price London–New York was roughly 10,000 dollars compared to 8,000 dollars for first class and 5,000 dollars for business class tickets of subsonic airliners" [25]. It thus became

[1] Assuming that a supersonic aircraft could fly twice as fast as a subsonic aircraft, it would be possible to replace two conventional aircraft, thus reducing maintenance and personnel costs.

a symbol, as it was designed in such a way that it was well ahead of its time. Despite this, the *Aérospatiale-BAC Concorde* had certain limitations: it was characterised by limited fuel economy, high maintenance and, above all, an engine that was too noisy during take off and significant pollutant emissions.
These conditions have thus contributed to the decline of commercial aircraft, despite their great advantage in offering shorter travel times. As a result, in recent times, there has been renewed interest in flying beyond the speed of sound, driven by technological advances in aerodynamics, propulsion, structure and control.

- Aerodynamics: the aircraft geometry capable of handling shock waves and minimising drag.
- Propulsion: the jet engine capable of effectively compressing and heating the air to produce the necessary thrust.
- Structure: advanced materials capable of withstanding the high temperatures generated by aerodynamic heating.
- Control: control systems capable of managing flight conditions and aerodynamic instabilities.

More and more efficient and environmentally friendly aircraft concepts are under consideration, making the future revival of supersonic flight promising. One of the most important contemporary examples is the *Boom Overture*, an airliner that will theoretically be introduced in 2029, guaranteeing 500 routes with business class fares.
However, being a prototype that is not yet fully defined, there are still significant challenges to be met in the supersonic field in terms of:

- safety, where design, maintenance and pilot training must meet stringent standards;
- environmental impact, where high noise levels, fuel consumption and pollutant emissions are aspects that require necessary solutions.

In particular, the increase in pollutant emissions and the resulting climate change symbolise some of the most pressing threats today.
Within the transport sector, aviation contributes significantly to the release of carbon dioxide (CO_2), carbon monoxide (CO), nitrogen oxides (NO_x), unburned hydrocarbons (HC), particulate matter (PM) and water vapour, with effects not only on the environment but also on human health.
In response, in 2020 the European Union approved an action plan called the *Green Deal*, which aims to make Europe the first zero-emissions continent by 2050, keeping global warming below 2° C compared to pre-industrial levels.
This is putting the aviation sector under severe pressure. Indeed, the growing demand for air travel, linked to increasing population and prosperity, will lead to an ever-increasing increase in CO_2 emissions: "this surge in aviation demand is projected to result in 3.1 billion tons of GHG emissions by 2050, which is 4 times greater than the 2015 baseline of 0.78 billion tons" [3]. This

condition could only be mitigated through a combination of strategies aimed at optimising routes, improving aerodynamic, propulsive and structural efficiency, and decreasing the use of fossil fuels. To date, attempts to improve technologies have begun to ensure the reduction of greenhouse gas emissions through lighter and stronger materials and increasingly efficient engines: "for example, 15 billion liters of fuel, and 80 million tons of CO_2, were saved by retro-fitting wing tip devices to the wings of over 5,000 existing aircraft (ATAG, 2019). By also using weight reduction measures on cargo containers, GHG emissions decreased by 10,000 t/year (ATAG, 2014)" [3].
According to the European Union, the concept of sustainability is increasingly important so that advanced and innovative aviation solutions can be researched and developed in the form of electric and hybrid aircraft, as well as biofuels. In this regard, according to the ICAO (*International Civil Aviation Organisation*), "SAF should achieve life cycle emission reductions of at least 10% compared to a fossil fuel baseline of 89 grams of CO_2 gCO_2/MJ" [24].

1.2 Conceptual Design

Aircraft design is usually conducted by implementing an iterative and recursive process that requires close collaboration between experts, attention to detail and compliance with safety regulations.
Starting with the definition of the high-level requirements based on the performance and characteristics desired by the customer, the process is divided into three main phases: conceptual, preliminary and detailed (Figure 1.1).
During the first one, the basic aircraft concept is developed, examining different layouts, configurations and solutions, and taking into account aerodynamic, propulsion, structural and economic aspects.
During the second one, the selected concept is refined, defining subsystem characteristics and evaluating load distribution, centre of gravity, stability and manoeuvrability.
During the third one, the concept is detailed, defining the specifications of each component.

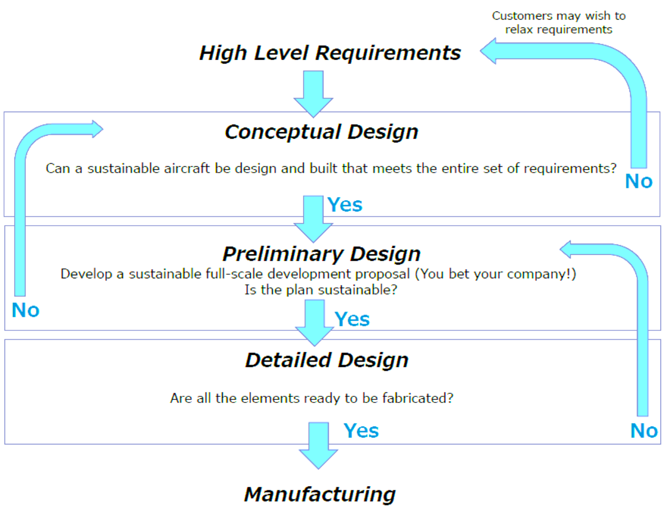

Figure 1.1: Design Process

In particular, conceptual design is the most important step in the iterative process.
It is an initial and high-level life cycle activity aimed at identifying a problem, determining the associated need and developing a configuration to meet the requirements sought.
This phase is characterised by continuous and evolutionary changes in aeronautical concepts, both to incorporate new knowledge and to evaluate potential improvements, analysing each time the variations that arise in terms of performance, weights and dimensions. In this way, it is possible to arrive at a final solution that can be refined during subsequent design stages [20, 23].

1.2.1 Models Proposed in the Literature

Conceptual design, when applied in relation to the environmental aspect, tends to consider two fundamental variables: noise and emissions generated by propulsive motion.
In this regard, the literature has tried its hand at several occasions, but has not provided sufficiently significant data.
An investigation conducted by Stanford University, California, and the Institute of Technology in Cambridge, Massachusetts, proposed the development of a medium to long range supersonic aircraft. The design tool consisted of a set of algorithms, useful for calculating design and performance aspects. Specifically, in terms of noise, the research was based on the use of ANOPP (*Aircraft Noise Prediction Program*), a semi-empirical code capable of incorporating publicly available prediction schemes continuously updated by NASA (*National Aeronautics and Space Administration*). Three noise sources were considered, namely fan, jet and airframe, while other sources such as the combustor, turbines and compressors were not analysed, as they have a negligible impact on the total aircraft noise.

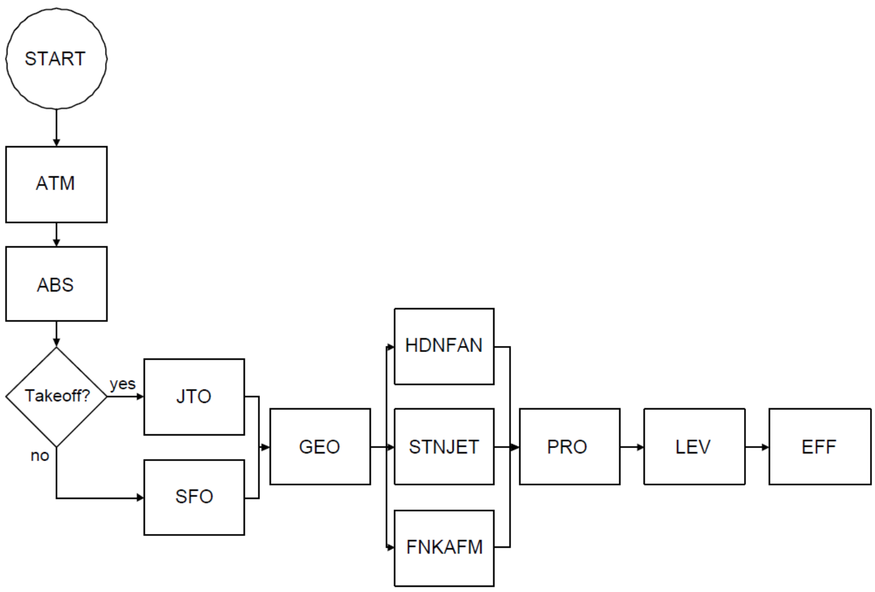

Figure 1.2: ANOPP Program Modules

As the picture shows, the process began with the definition of the atmospheric pattern (ATM) and the relative absorption (ABS). "The steady flyover module (SFO) is used for the approach measurement point, and the jet takeoff module (JTO) for sideline and takeoff measurement points. The

geometry module (GEO)" was useful to calculate "the range and directivity angles from the observer to the noise source". The sources considered related to the models of "Heidmann for fan noise (HDNFAN), Stone for coaxial jet noise (STNJET) and Fink for airframe noise (FNKAFM)" [2]. The collected data were then subjected to corrections through the last three modules, in order to be transferred to the observer's reference system, considering atmospheric absorption effects.
Regarding emissions, although the ICAO regulations for the LTO (*Landing Take Off*) cycle mention CO, NO_x and HC, the American study only analysed the release of nitrogen oxides, which were calculated based on the engine's fuel flow rate and the combustor's emission index using the following formula:

$$LTO\ NO_x = \sum Fuel\ Flow \cdot Emission\ Index_{NO_x} \cdot Time\ in\ Mode$$

The literature proposes other similar models, such as that analysed by Cranfield University, UK, again based on semi-empirical noise prediction algorithms. Similarly to the research mentioned above, the following investigation examined fan noise, but through the formulation derived from Gliebe, and airframe noise, again using Fink's method. In contrast, combustor noise, implementing the SAE ARP876 standard, and turbine noise, using the method proposed by Krejsa and Valerino, were considered. However, the study did not monitor the incidence of pollutant emissions from the observed aircraft [10].

An innovative proposal developed instead in the Italian context is ASTRID (*Aircraft on board Systems sizing and TRade off analysis in Initial Design*), a software conceived by the research group of the Department of Mechanical and Aerospace Engineering of the Polytechnic of Turin. It provides a working environment for the conceptual and preliminary design of conventional and innovative aircraft configurations for the subsonic and low supersonic regime.
Even more recent is the new ASTRID-H software, which extends ASTRID's domain to supersonic and hypersonic. Its objective is to support users in the translation of data which, from statistical and design evaluation, can be converted into the aircraft geometry. "Already available and widely used mathematical models are here integrated in a new algorithm to face the complexity of the design of high-speed vehicles" [5]: this is achieved through a high level of integration between the airframe and the impact subsystems, without the possibility of carrying out the preliminary design activities in series. More specifically, this program consists of five complementary routines: estimation of selected data, definition of the design space, feasibility analysis of mass and volume, decomposition of variables from the previous phase, and 3D CAD modelling of the aircraft and its subsystems.

1.2.2 Model Under Analysis

The case study presented here proposes to offer a more innovative point of view than the aforementioned attempts, symbolising an important resource for the development of MORE&LESS (*MDO and REgulations for Low-boom and Environmentally Sustainable Supersonic aviation*), a

European project aimed at the definition of global environmental regulations for future supersonic aviation, and for the refinement of ASTRID-H.
In fact, the methodological process in question aims to extend the design domain to supersonic aircraft, similar to ASTRID-H, but appropriately integrating sustainable numerical algorithms for the dimensioning of aircraft with low environmental impact. The project's mission is therefore oriented not only towards operational requirements, but also towards ecological LTO cycle requirements during aircraft design.

In the case analysed here, the methodology adopts a simplified statistical approach to the assessment of noise and pollutant emission levels, thus going beyond the criteria considered so far in the literature.
This type of investigation in fact makes it possible to examine effectively quantifiable experimental data and thus establish analytical relations between them, producing numerical results that can be easily integrated within the Matching Chart. In this way, the data, although not perfectly accurate, enhances the identification of the design point.

More specifically, in terms of emissions, whereas in general they are only weighted about NO_x, in this new approach, emissions of nitrogen oxides, carbon monoxide and unburned hydrocarbons are also assessed, as stated in the ICAO regulations.

Based on these considerations, it emerges that the transition to high-speed, low environmental impact aircraft is essential to offer a solution characterised by reduced mission times and high efficiency, contributing to the creation of a more connected and sustainable future for the aviation industry and the entire planet.
Therefore, using a multidisciplinary approach, the following research aims to define a conceptual design methodology for the development of a sustainable supersonic commercial aircraft, operating in the cruise condition at Mach 2 and powered by biofuel. The objective is to meet high-level requirements while ensuring a technically feasible and commercially viable realisation in a future perspective.

Consequently, since ASTRID-H is not a fully refined software, it is convenient that the procedures and formulations are implemented in a programming language such as Python, which is object-oriented and particularly suitable for the realisation of applications.
The case study focuses on satisfying specific design constraints.

- Cruising Mach: 2
  Achieving supersonic speed implies the necessary adoption of an extremely slender layout, capable of optimising the lift-to-drag ratio.

- Passengers: 100
  The size of the payload, roughly comparable to that of the *Aérospatiale-BAC Concorde*, is

functional to maximise occupancy on board and minimise the overall operating costs[2], thus offering affordable and competitive fares.

- Range: 6000 km
  The range cannot be excessive due to the high fuel consumption caused by viscous and aerodynamic drag.

- Propellant: biofuel
  The use of a biofuel source does not affect the aircraft design, as it does not require any modifications to the fuel system, but provides a significant environmental benefit.

Specifically, the methodology proposed below is based on the implementation of an approach aimed at determining a design point capable of meeting precise operational and environmental requirements, estimating the performance and geometric characteristics of the aircraft, and evaluating the biological propellant type. The *Aérospatiale-BAC Concorde* is taken as a reference in several aspects of the discussion.
It consists of several steps[3].

1. Creation of the statistical database: is a starting point for an initial sizing estimation, taking into account a set of reference civil supersonic aircraft.

2. Calculation of the initial sizing: leads to a first attempt solution of the performance and geometric properties of the aircraft.

3. Definition of the mission profile: provides a detailed picture of the activities and operations that an aircraft performs during its operational life.

4. Description of the aerodynamic model: develops an advanced synthesis of scientific theories and experimental data, resulting in a system of analytical equations capable of evaluating aircraft behaviour.

5. Initialisation of the iterative cycle: allows a refinement of the maximum take off mass concept.

6. Elaboration of the Matching Chart: graphically illustrates the operational and environmental constraints during mission execution to outline a feasible design space and optimal design point.

7. Calculation of the updated sizing: refines the initial configuration to revise performance and geometric characteristics.

8. Investigation of biofuel properties: offers a transformation of the aviation sector towards ecological sustainability by monitoring CO_2 emissions, assessing costs and proposing considerations for the future.

[2]The use of a homogeneous and smaller fleet of aircraft simplifies maintenance and reduces associated costs.
[3]The algorithms in Python follow this order of presentation, although the last step is not implemented directly as the biofuel is irrelevant to the aircraft design.

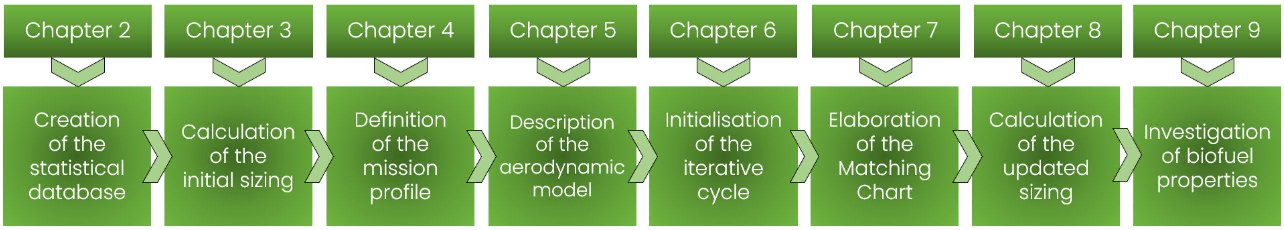

Figure 1.3: Flowchart

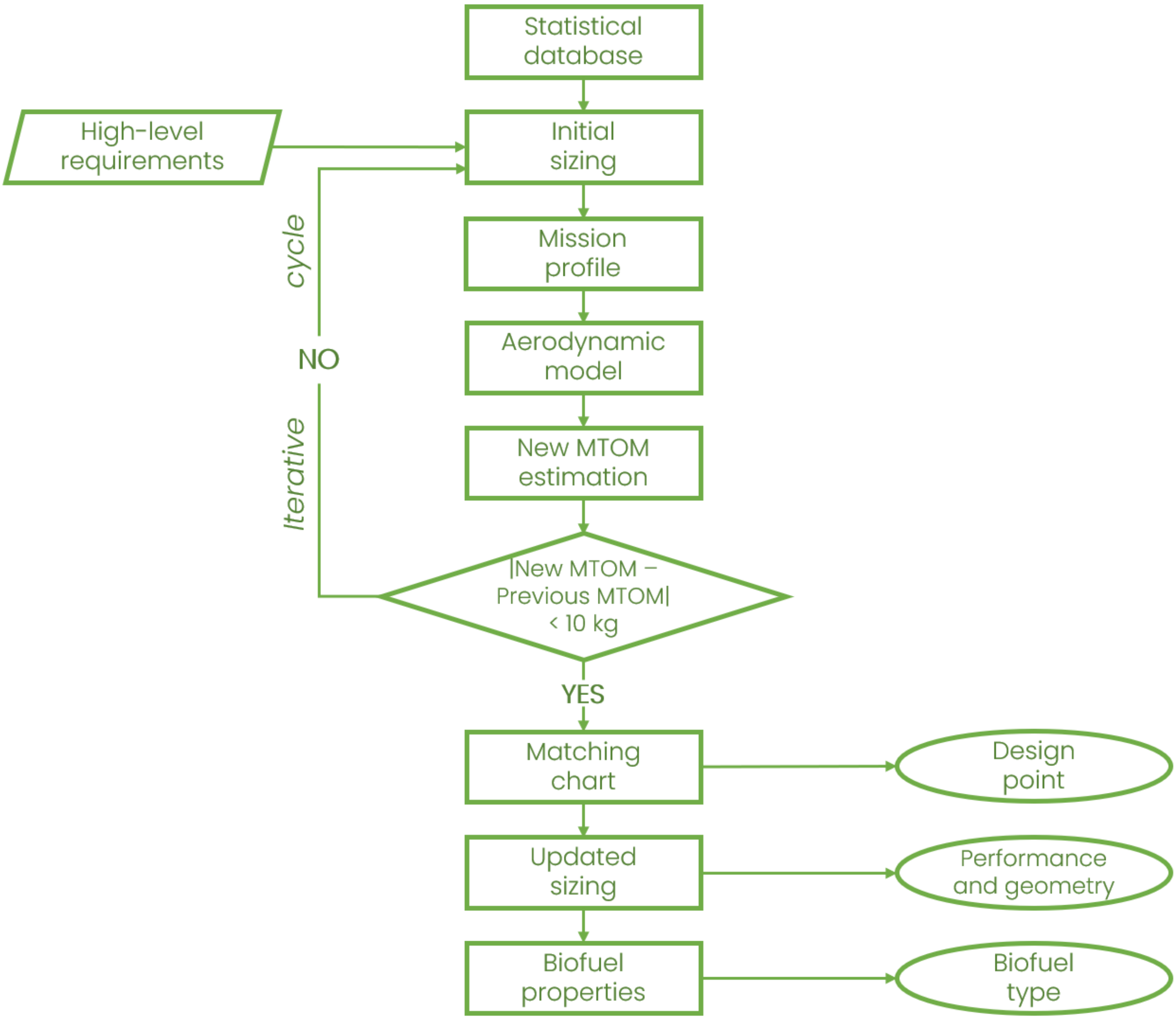

Figure 1.4: Flowchart

1.3 Regulations

This project, as previously mentioned, is being developed in accordance with ICAO regulations, which regulate, among other issues, the limitation of the impact of aircraft on the environment.
The Organisation first related to the concept of noise in 1971, through specific regulations designed for subsonic aircraft. Subsequently, the regulations were extended in 1981 to high-speed transport, specifying maximum noise levels for the first examples, such as the *Aérospatiale-BAC Concorde*. The framework remained unchanged for decades, until new supersonic alternatives were proposed in 2010 for business jets and commercial jets.
As these aircraft were small, the absolute levels of take off and landing noise and emissions were lower than those of larger aircraft. Precisely with regard to emissions, the ICAO initially expressed its opinion with a small study group, from 1973 to 1977, and then with a committee, from 1978 to 1980, focusing on turbojet and turbofan engines for commercial aviation. The outcome of the research bore fruit, as an international certification test and a measurement model capable of monitoring emissions of carbon monoxide, nitrogen oxides and unburned hydrocarbons was introduced.
However, as studies on the subject are still not exhaustive, the ICAO-CAEP (*Committee for Aviation Environmental Protection*) has set itself the challenge of analysing noise and emission characteristics in more detail for the development of innovative certification standards in the future. Obviously, these must be technically feasible, i.e. implementable through compliance with the levels of technology that have been achieved until that moment. In this way, as new environmental challenges increase, the Organisation has the possibility of increasing the severity of the provisions through certification limits at periodic intervals.

The analysis carried out here has been specifically compared, firstly, with *Annex 16 - Environmental Protection, Volume I - Aircraft Noise*, which, with regard to noise, defines the maximum noise levels of supersonic aircraft (regulated in Chapter 12). However, they are not specifically defined, but simply refer to the maximum levels of subsonic aircraft (regulated in Chapter 14), albeit only with reference to the LTO cycle and not the cruise phase. As can be seen from the regulations: "Standards and Recommended Practices for these aeroplanes have not been developed. However, the maximum noise levels of the Part that would be applicable to subsonic jet aeroplanes may be used as a guideline. Acceptable levels of sonic boom have not been established and compliance with subsonic noise Standards may not be presumed to permit supersonic flight" [12]. In fact, supersonic overflights of continental areas are prohibited for civil purposes, with the consequence that high-speed transport could only follow a coherent motion on trajectories over the sea, such as the transatlantic or transpacific routes.
According to this standard, the sum of the differences between the maximum permissible noise levels and those effectively perceived at three measurement points (Approach, Flyover, Lateral) must not be less than 17 dB. Specifically, the EPNL (*Effective Perceived Noise Level*) assesses the annoyance caused to individuals by "aircraft noise, which has unique spectral properties and a persistent soundscape. It takes into account how people react to the spectral structure, intensity,

tonal content, and duration of aircraft noise" [10].

$$[(LIMIT_A - EPNL_A) + (LIMIT_F - EPNL_F) + (LIMIT_L - EPNL_L)] \geq 17 \tag{1.1}$$

Where maximum levels can be quantified by the reference below.

M = Maximum take-off mass in 1 000 kg		0	2	8.618	20.234	28.615	35	48.125	280	385	400
Lateral full-power noise level (EPNdB) All aeroplanes		88.6	86.03754 + 8.512295 log M	94			80.86511 + 8.50668 log M				103
Approach noise level (EPNdB) All aeroplanes		93.1	90.77481 + 7.72412 log M	98			86.03167 + 7.75117 log M		105		
Flyover noise levels (EPNdB)	2 engines or less	80.6	76.57059 + 13.28771 log M	89				66.64514 + 13.28771 log M		101	
	3 engines			89		69.64514 + 13.28771 log M				104	
	4 engines or more			89	71.64514 + 13.28771 log M					106	

Figure 1.5: Maximum Permissible Noise Levels

Emissions, on the other hand, have been addressed through *Annex 16 - Environmental Protection, Volume II - Aircraft Engine Emissions*, in which the maximum pollutant levels of supersonic aircraft (regulated in Chapter 3) are specifically defined, albeit only with reference to the LTO cycle and not the cruise phase, in terms of the release of carbon monoxide, nitrogen oxides and unburned hydrocarbons depending on the engine type [11].

$$CO = 4550(\pi_\infty)^{-1.03} \tag{1.2}$$

$$NO_x = 36 + 2.42\pi_\infty \tag{1.3}$$

$$HC = 140(0.92)^{\pi_\infty} \tag{1.4}$$

Where π_∞ denotes the ratio of the mean total pressure, at the last compressor discharge plane of the compressor, to the mean total pressure, at the compressor entry plane, when the engine is developing take off thrust rating in ISA sea level static conditions.

These elements will be of crucial importance in the processing of the Matching Chart.

Chapter 2

Statistical Database

A statistical database represents a tool for confirming the requirements introduced in the previous chapter, as well as a starting point for estimating an initial sizing.
It must therefore be composed of a set of reference civil supersonic aircraft, developed through engineering programs that have resulted in an advanced concept, a prototype or even an operational version of the aircraft, and whose properties are identified by means of a literature review, carried out using on-line searches and technical documents.

2.1 Candidate Family

The candidate family consists of:

- Lockheed L-2000;
- Boeing 2707;
- Tupolev TU-144;
- Aérospatiale-BAC Concorde;
- Tupolev TU-244;
- NASA Concept Mach 2.7;
- NASA Concept Mach 3;
- NASA 1st Concept Mach 2.4;
- NASA 2nd Concept Mach 2.4;
- Tupolev TU-444;
- Aerion SBJ;
- Spike S-512;

- Boom XB-1;
- Boom Overture.

Lockheed L-2000

The *Lockheed L-2000* could have been a competitor to the Anglo-French *Aérospatiale-BAC Concorde* program and the Soviet *Tupolev Tu-144* program, but the *Boeing 2707* won the contract awarded by the US government.
The concept, developed by the *Lockheed Corporation* of the same name, envisaged the construction of a supersonic aircraft, capable of operating up to a cruising speed of Mach 3, carrying up to 273 passengers and characterised by a slightly curved streamlined nose and a double delta wing.

Figure 2.1: Lockheed L-2000

Boeing 2707

The *Boeing 2707* was intended as a rival to the Anglo-French *Aérospatiale-BAC Concorde* program and the Soviet *Tupolev Tu-144* program, but high costs and uncertain economic returns led to the cancellation of the program before the two prototypes were completed.
The concept, developed by the *Boeing Company* of the same name, envisaged the construction of a supersonic aircraft, capable of operating up to a cruising speed of Mach 2.7, carrying up to 234 passengers and initially featuring a variable geometry wing and later a delta wing.
The development program began in 1963 and ended in 1971.

Figure 2.2: Boeing 2707

Tupolev Tu-144

The *Tupolev Tu-144* or *Concordski* represents a supersonic airliner in service since 1968, but only until 1998 due to technical problems, economic limitations and political changes.
The concept, designed by the *Tupolev Company* of the same name, bore a strong resemblance to the *Aérospatiale-BAC Concorde*, albeit with significant differences in controls, navigation and engines: both possessed the unique ability to change the position of the nose cone depending on the phase of flight, but the former had a double delta wing with conical curvature and two small canard surfaces to increase lift at low speed, thus reducing the space required for take off and landing.
The *Concordski* operated at a slightly variable cruising speed around Mach 2, with a transport capacity of up to 150 passengers, depending on the engine installed and the type of version: 144, 144S, 144D and 144LL.

Figure 2.3: Tupolev Tu-144

Aérospatiale-BAC Concorde

The *Aérospatiale-BAC Concorde* represents a supersonic airliner in service since 1976, but only until 2003 due to its high fuel consumption and significant maintenance costs.
The concept, developed by the Anglo-French consortium formed by *British Aerospace* and *Aérospatiale*, was characterised by a unique configuration for its time, which was no longer used due to technical-commercial choices that favored the construction of aircraft with a greater load capacity rather than greater speed. It possessed the extraordinary ability to change the position of the nose cone depending on the phase of flight, had an ogival delta wing with no horizontal tail planes, and operated at a cruising speed of Mach 2 with a transport capacity of up to 120 passengers.

Figure 2.4: Aérospatiale-BAC Concorde

Tupolev Tu-244

The *Tupolev Tu-244* was supposed to be the aeronautical technological evolution of the *Tupolev Tu-144*, using cryogenic fuel to increase the range in kilometres.
The concept, developed by the *Tupolev Company* of the same name, envisaged the creation of a supersonic aircraft with a non-tilting nose cone, giving the pilot a view captured by special cameras, capable of operating at a cruising speed of Mach 2.2 and with a transport capacity of up to 320 passengers.
Design began in 1979, but was abandoned in 1993 although flight tests were scheduled to begin in 2025.

Figure 2.5: Tupolev Tu-244

NASA Concept Mach 2.7

In 1985 *NASA* conceived of a Mach 2.7 supersonic aircraft, capable of flying non-stop from the Americas to many parts of Europe, Asia and Africa.
The concept involved a suitably designed and refined wing and canard surface [7].

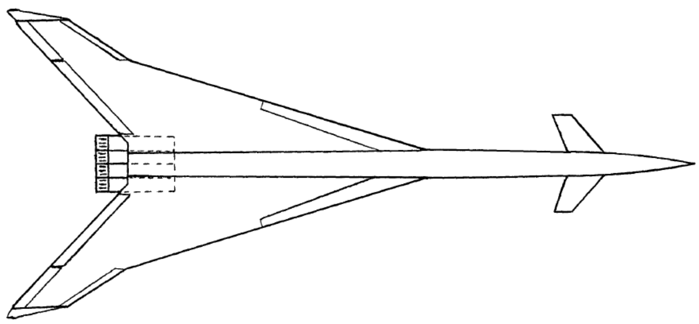

Figure 2.6: NASA Concept Mach 2.7

NASA Concept Mach 3

In 1988 *NASA* conceived of a Mach 3 supersonic aircraft, representing a threshold between the *wing-body* configuration, typical of supersonic flight, and *waverider*, typical of hypersonic flight. The concept involved the implementation of innovative aerodynamic, propulsion, structural and control aspects [21].

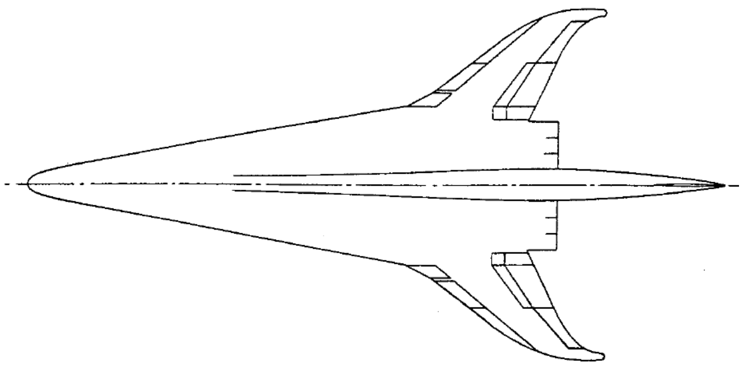

Figure 2.7: NASA Concept Mach 3

NASA 1st Concept Mach 2.4

In 1992 *NASA* designed the first Mach 2.4 supersonic transport, capable of halving the duration of international flights, while maintaining competitive comfort levels and minimal environmental impact.
The concept included a high-performance design, with variable geometry wingtips, the absence of a horizontal tailplane, the introduction of a synthetic system for both pilot and passenger external vision and the installation of a *fly-by-light* flight control system to cope with the instability of supersonic cruise [1].

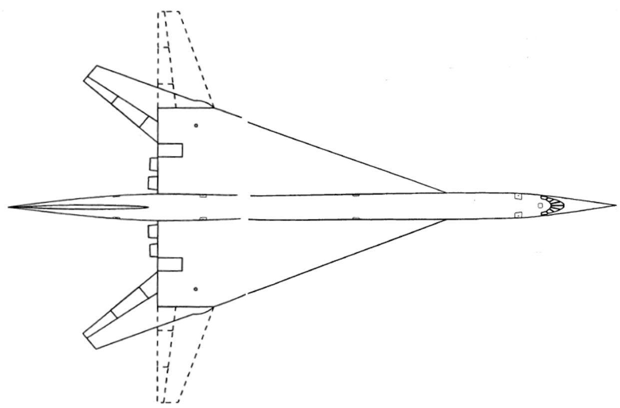

Figure 2.8: NASA 1st Concept Mach 2.4

NASA 2nd Concept Mach 2.4

In 1999 *NASA* designed the second Mach 2.4 supersonic transport, to serve as the basis for studies to evaluate the advanced technologies required for a possible future supersonic aircraft.
The concept included the design of a configuration characterised by high aerodynamic cruising efficiency and reduced weight through the removal of the horizontal tailplane [4].

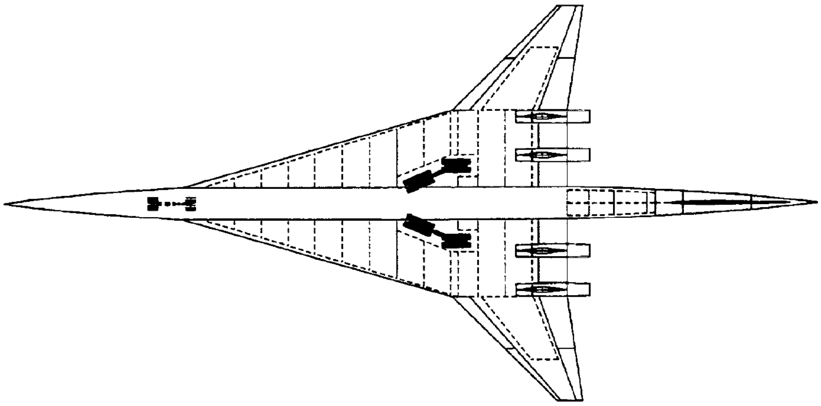

Figure 2.9: NASA 2nd Concept Mach 2.4

Tupolev Tu-444

The *Tupolev Tu-444* was intended to be a supersonic alternative to the *Tupolev Tu-244*, taking advantage of smaller dimensions and thus allowing a lower economic and environmental impact.
The concept, developed by the *Tupolev Company* of the same name, was to build the construction of a business jet, capable of operating at a cruising speed of Mach 2 and with a transport capacity of 6 to 10 passengers.
Design began in 2000, but the project gradually fell into oblivion and was eventually cancelled.

Figure 2.10: Tupolev Tu-444

Aerion SBJ

The *Aerion SBJ* was intended to be the first supersonic commercial aircraft after the retirement of the *Aérospatiale-BAC Concorde*, but a lack of new capital prevented its commercialisation.
The concept, developed by the *Aerion Corporation* of the same name, was to create a business jet, capable of operating at a cruising speed of Mach 1.7 and with a transport capacity of 8 to 12 passengers, depending on the configuration.
Flight tests began in 2013, in collaboration with *NASA*, and the first deliveries were scheduled to begin in 2023, in collaboration with *Airbus*.

Figure 2.11: Aerion SBJ

Spike S-512

The *Spike S-512* represents a supersonic business jet expected to be launched in 2024, providing short and long distance routes for private and business travellers.
The concept, developed by the *Spike Aerospace* company of the same name, identifies a windowless model, offering passengers a view captured by special cameras, capable of sustaining a cruising speed of Mach 1.6 and with a transport capacity of up to 18 passengers.

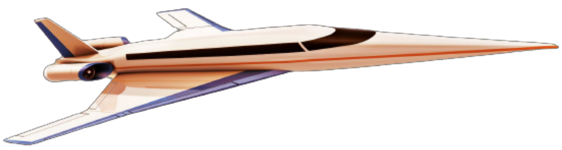

Figure 2.12: Spike S-512

Boom XB-1

The *Boom XB-1* or *Baby Boom* represents a supersonic demonstrator expected to be launched in 2024 as part of the development of the *Boom Overture* aircraft.
The concept, developed by *Boom Technology*, identifies a 33% scale model of the *Boom Overture*, capable of sustaining a cruising speed of Mach 2.2 and equipped with a two-member cockpit with no possibility of accommodating additional passengers.

Figure 2.13: Boom XB-1

Boom Overture

The *Boom Overture* represents a supersonic aircraft expected to be launched in 2029, with flights starting in 2030 and providing 500 viable routes with business class fares.
The concept, developed by *Boom Technology*, identifies a 75% scale model of the *Aérospatiale-BAC Concorde*, but at a quarter of the cost thanks to the introduction of advanced technologies, delta wings, afterburner-free engines and composite structures, offering low drag, as well as a cruising speed of Mach 1.7 and a transport capacity of up to 88 passengers.

Figure 2.14: Boom Overture

2.2 Performance and Geometric Characteristics

The performance and geometric characteristics of the previously described aircraft models are summarised here.

Aircraft	Mach	Passengers	Range	OEM	Payload	Fuel	MTOM	Thrust	SFC
L-2000	3	273	7400	107955	25000	134664	267619	1160	5.00E-05
2707	2.7	234	6685	98010	22185	220000	340195	1164	5.00E-05
TU-144	2.17	150	2920	98000	12000	70000	180000	688	5.10E-05
TU-144S	2.07	150	3600	82000	15000	98000	195000	712	5.10E-05
TU-144D	2	150	6200	99000	15000	93000	207000	784	3.50E-05
TU-144LL	2.17	150	4000	93000	15000	95000	203000	980	4.80E-05
Concorde	2.04	120	6230	76690	12700	95680	185070	676	3.60E-05
TU-244	2.2	320	9200	143200	28800	178000	350000	1295	4.80E-05
NASA 2.7	2.7	300	11112	125914	32220	153575	311709	854	5.10E-05
NASA 3	3	250	12038	119594	29092	175041	323727	1635.3	5.10E-05
NASA 1st 2.4	2.4	294	10649	156338	26460	194591	377389	1340	2.80E-05
NASA 2nd 2.4	2.4	251	12038	86851	28430	163361	278642	800.8	2.80E-05
TU-444	2	10	7500	19500	1000	20500	41000	190	5.60E-05
SBJ	1.7	12	7800	19230	1000	20593	40823	174	2.20E-05
S-512	1.6	18	11500	24041	2722	25400	52163	178	2.20E-05
XB-1	2.2	0	1900	2538	520	3065	6123	57	6.00E-05
Overture	1.7	88	7870	32011	6500	38600	77111	640	3.00E-05

Table 2.1: Performance Characteristics

Aircraft	Fuselage Length	Fuselage Width	Fuselage Height	Aircraft Height
L-2000	83.26	4.99	4.69	14
2707	91.44	3.72	4.21	16.17
TU-144	59.4	3.5	3.25	12.25
TU-144S	65.7	3.45	3.5	14.4
TU-144D	65.7	3.45	3.5	14.4
TU-144LL	65.7	3.45	3.5	14.4
Concorde	61.66	2.9	3.08	12.2
TU-244	88.7	3.9	4.11	16.9
NASA 2.7	81.08	2.67	3.04	12.56
NASA 3	90.83	2.33	2.65	10.97
NASA 1st 2.4	94.49	4.01	4.57	18.9
NASA 2nd 2.4	91.44	3	3.43	14.17
TU-444	36	2.16	2.28	6.51
SBJ	41.33	2.14	2.26	6.46
S-512	37	2.06	2.17	6.2
XB-1	20.7	1.23	1.31	5.2
Overture	61	2.62	2.78	11

Table 2.2: Fuselage Characteristics

Aircraft	Area	Span	Root Chord	Tip Chord	Mean Sweep Angle
L-2000	875.5	35.36	51.35	3.08	75
2707	865.6	43.72	56.4	3.38	63
TU-144	438	27.65	30.29	1.82	67
TU-144S	503	28	33.5	2.01	67
TU-144D	507	28.8	33.5	2.01	67
TU-144LL	507	28.8	33.5	2.01	67
Concorde	358.25	25.6	27.71	1.66	55
TU-244	1200	54.77	54.71	3.28	63
NASA 2.7	919.74	39.62	43.74	7.32	66
NASA 3	1132	45.72	56.02	3.36	66
NASA 1st 2.4	887.97	43.89	50.29	3.05	45
NASA 2nd 2.4	952.26	44.68	49.66	2.83	60
TU-444	136	16.2	18.36	1.1	67
SBJ	111.5	19.58	21.08	1.26	63
S-512	112.5	18	18.87	1.13	63
XB-1	63	5.2	10.55	0.63	55
Overture	218	18	31.1	1.87	55

Table 2.3: Wing Characteristics

Aircraft	Area	Span	Root Chord	Tip Chord	Mean Sweep Angle
L-2000	92.26	6.32	13.78	4.6	55
2707	151.1	10.35	15.25	3.05	45
TU-144	96.35	6.6	13.75	2.75	63.75
TU-144S	106.57	7.3	15.2	3.05	63.75
TU-144D	106.57	7.3	15.2	3.05	63.75
TU-144LL	106.57	7.3	15.2	3.05	63.75
Concorde	43.26	5.36	13.4	2.68	67.5
TU-244	107	7.33	13.2	2.92	43
NASA 2.7	27.87	2.82	7.32	1.82	67
NASA 3	12.23	2.44	8.38	1.65	70.1
NASA 1st 2.4	102.19	7	20.72	6.1	67.5
NASA 2nd 2.4	41.81	5.18	13.44	2.68	60
TU-444	34	3.44	5	1.55	43
SBJ	11.12	2.22	8.58	5.4	70
S-512	32.12	3.25	5.32	2.32	45
XB-1	8.07	1.61	4.42	0.8	67.5
Overture	38.26	4.74	13.02	2.36	67.5

Table 2.4: Tail Characteristics

The units of measurement for the various quantities are specified in detail in the next chapter.

Chapter 3

Initial Sizing

The initial sizing symbolises a first attempt at the performance and geometric properties, assumed by the sustainable supersonic aircraft in question.
The numerical results obtainable identify a first step towards the definition of a technically feasible and commercially viable aeronautical configuration, proposing a rough layout that can be improved by applying more detailed methodologies in subsequent phases.
Preliminary sizing can be achieved by means of a statistical approach based on determining the linear regression between an input quantity and an output quantity (Figure 3.1).
Starting from the value of a known variable on the x-axis, it is thus possible to determine the value of an unknown variable on the y-axis by intersecting the linear trend that correlates the two entities.

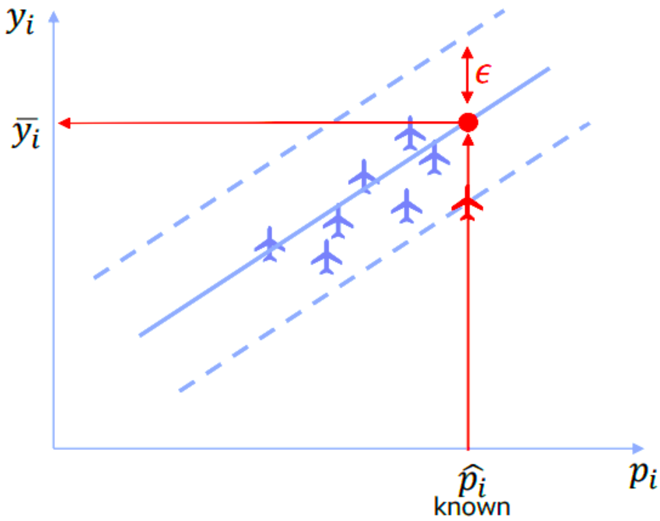

Figure 3.1: Statistical Approach

By introducing the high-level requirements, it is therefore possible to identify the measure of the main aircraft characteristics based on the statistical family previously identified and the approach proposed in the figure below.

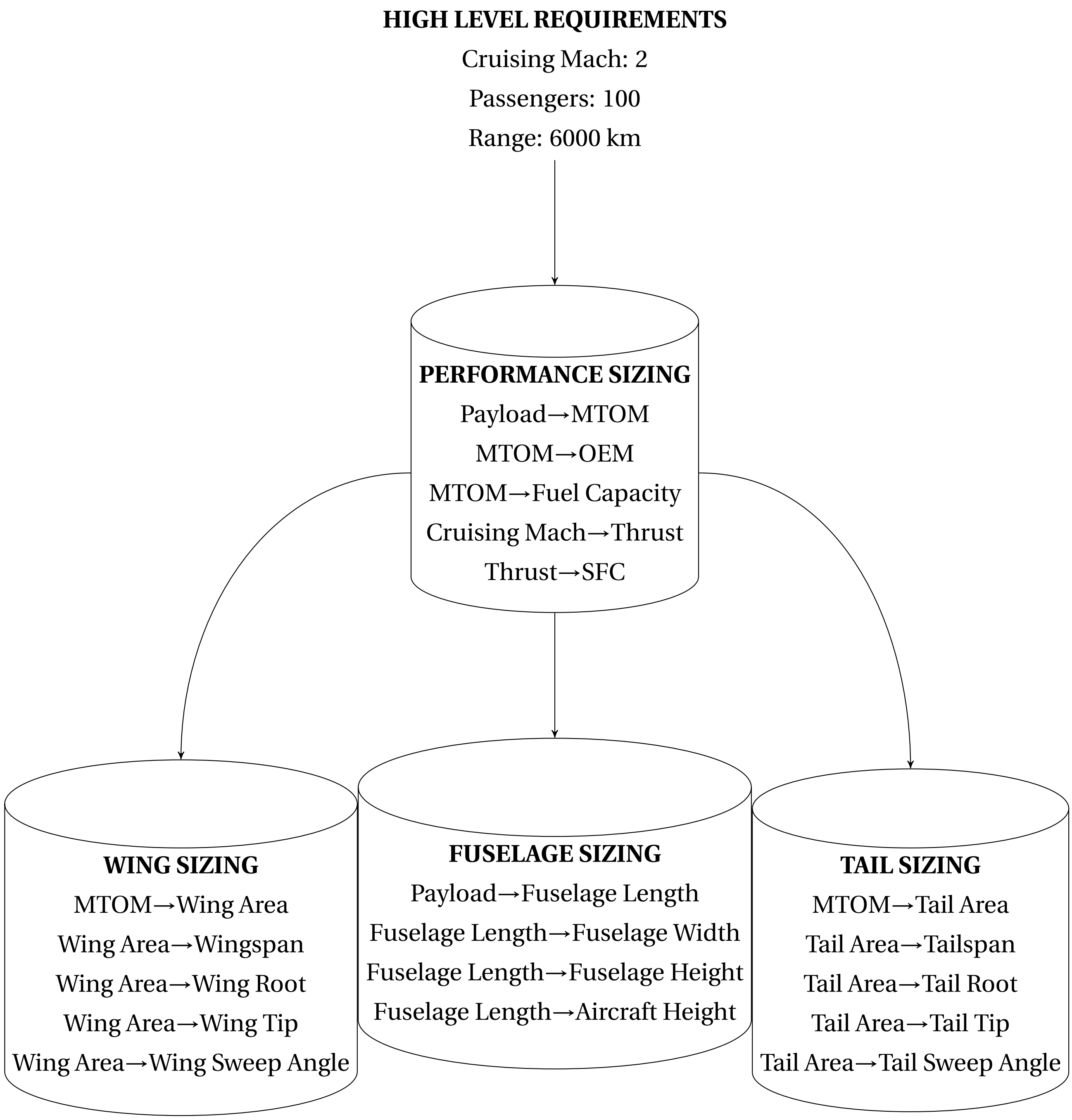

Figure 3.2: Statistical Approach

The results are summarised here[1], where aspect ratio, mean aerodynamic chord and taper ratio are respectively quantified as:

$$AR = \frac{b^2}{S}$$

$$MAC = \frac{2}{3}\frac{c_r^2 + c_r c_t + c_t^2}{c_r + c_t}$$

$$\lambda = \frac{c_t}{c_r}$$

[1]The payload can be calculated as the product of the number of passengers and 120 kg, which is the sum of the mass of each passenger and their luggage.

OEM [kg]	Payload [kg]	Fuel [kg]	MTOM [kg]	Thrust [kN]	SFC [kg/(N*s)]
65789.17	12000	80946.14	159087.63	597.74	4.1e-05

Table 3.1: Performance Sizing

Fuselage Length [m]	Fuselage Width [m]	Fuselage Height [m]	Aircraft Height [m]
58.92	2.81	2.94	10.95

Table 3.2: Fuselage Sizing

Area [m^2]	Span [m]	AR [-]	Root Chord [m]	Tip Chord [m]	MAC [m]	λ [-]	Mean Sweep Angle [deg]
447.57	26.5	1.57	31.76	2.09	21.26	0.07	62.31

Table 3.3: Wing Sizing

Area [m^2]	Span [m]	AR [-]	Root Chord [m]	Tip Chord [m]	MAC [m]	λ [-]	Mean Sweep Angle [deg]
57.24	4.88	0.42	11.17	2.83	7.83	0.25	60.82

Table 3.4: Tail Sizing

From a geometric point of view, it is useful to provide an approximate configuration of the aircraft to facilitate the understanding of the calculated structural model, also examining the surface level of the sections along the longitudinal axis and the amount of total volume.

Following the proportions of the *Aérospatiale-BAC Concorde*, the references below are adopted:

- nose development up to 15% of the fuselage length;
- tail cone development starting from 80% of the fuselage length;
- wing leading edge development starting from 25% of the fuselage length;
- tail leading edge development starting from 70% of the fuselage length;
- wing and tail conformation assessed by considering span, chord at root and chord at tip, and disregarding area, mean sweep angle, dihedral angle and twist.

The top and side views can then be presented (Figure 3.3), also introducing the relative Mach cone angle generated by the supersonic motion calculated as:

$$\mu = \arcsin \frac{1}{M}$$

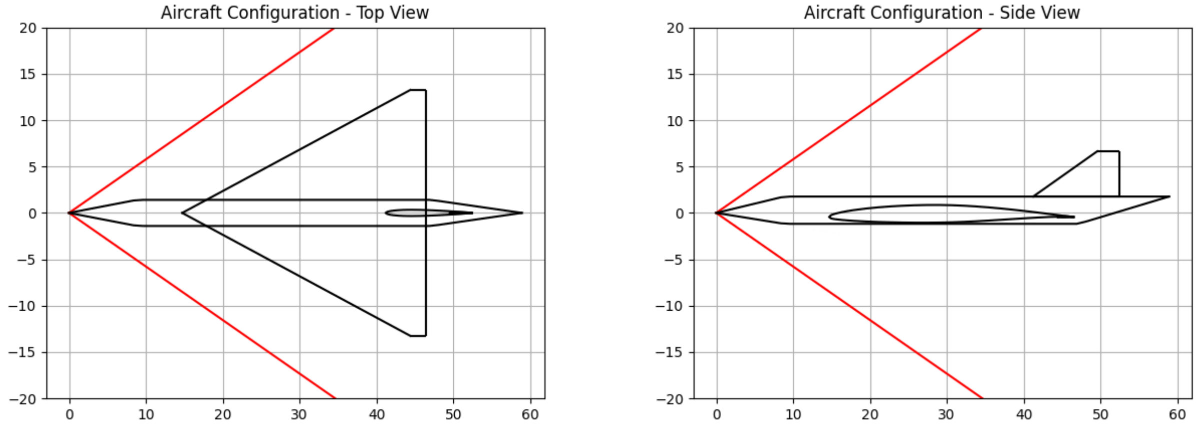

(a) Top View (b) Side View

Figure 3.3: Configuration

This geometry results in a distribution of section areas that obviously deviates from the optimal *Sears-Haack* pattern governed by Equations 3.1 and 3.2, implying greater wave resistance and consequently reduced flight performance.

$$V = \frac{3\pi^2}{16} R_{max}^2 L \tag{3.1}$$

$$A(x) = \frac{16V}{3L\pi} [4x(1-x)]^{3/2} \tag{3.2}$$

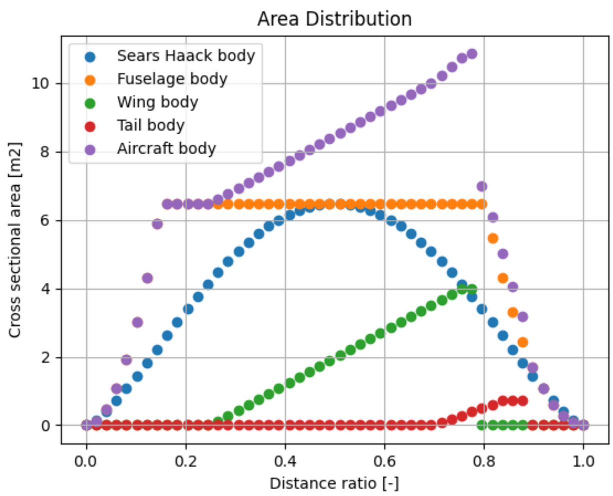

Figure 3.4: Area Distribution

In terms of volume, the value goes from 225 m^3, for the *Sears-Haack* body, to 365 m^3, for the real body, confirming once again the non-optimality of the geometric solution.
In any case, at this point it is essential to refine the numerical results obtained.

Chapter 4

Mission Profile

The mission profile provides a detailed picture of the activities and operations that an aircraft will be expected to perform during its operational life, providing a further foundation on which the design process is based.
From the moment of take off to landing, the profile takes into account several crucial factors, in terms of range and operational altitude, appropriately calibrated to ensure performance, reliability and safety at the same time.
In fact, the aim is to optimise the flight path, maximising efficiency and reducing fuel consumption, hence, pollutant emissions, by favoring high altitudes, as the air is less dense, colder and at lower pressure, thus ensuring better propulsive performance.
Typically, the ideal cruising altitude is lower than the altitude at which the lift-to-drag ratio assumes its maximum value: in fact, although propellant consumption increases below the minimum drag altitude, the engine's required displacement and its installation weight decrease. The altitude at which these effects offset each other can be assumed to be the optimal one [25].

In light of these reflections, it is necessary to outline a plausible and realistic mission profile, taking inspiration from the *Aérospatiale-BAC Concorde*, the most concrete reference and most similar to the aircraft under study.
To this end, it is convenient to carry out a parameterisation[1] of its trajectory, in order to obtain the percentage fractions of each individual phase which, multiplied by the overall range of 6000 km, allow the kilometer contribution of each flight condition to be established.
Specifically, we consider a mission profile[2] that includes the *Missed Approach*, a missed approach procedure that guarantees the maintenance of minimum separation from obstacles through a climb, a holding, a descent and a final landing.

[1]The parameterisation is carried out by relating, phase by phase, the partial route to the total range of the *Aérospatiale-BAC Concorde*.
[2]The altitude of the departure and arrival airports is assumed to be 100 m and 50 m above sea level respectively.

Phase	Range [km]	Initial Altitude [m]	Final Altitude [m]
Take Off	2.83	100	110
Subsonic Climb	125	110	12000
Subsonic Cruise	600	12000	12000
Supersonic Climb	166.67	12000	18000
Supersonic Cruise	4204.16	18000	18000
Supersonic Descent	433.33	18000	12000
Subsonic Descent	341.67	12000	200
Climb	41.67	200	2000
Holding	61.67	2000	2000
Descent	20.83	2000	65
Landing	2.17	65	50

Table 4.1: Mission Profile

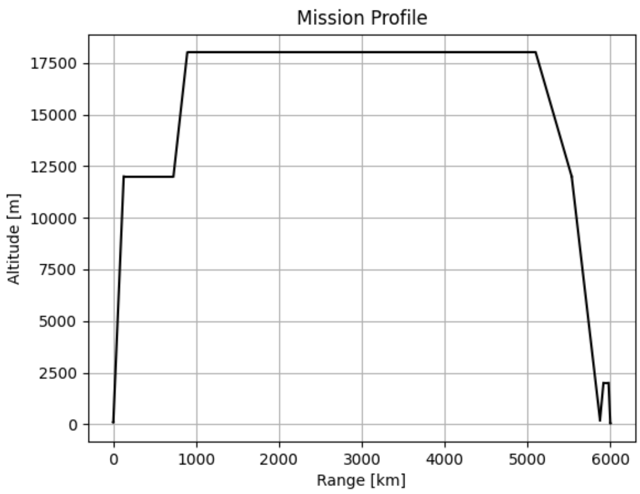

Figure 4.1: Mission Profile

Chapter 5

Aerodynamic Model

The aerodynamic model outlines an advanced synthesis of scientific theories and experimental data, resulting in a system of analytical equations capable of assessing the aircraft behaviour.
It takes into account several factors that influence the interaction between an aircraft and the surrounding air throughout the entire mission profile, including body shape, speed, altitude and angle of incidence[1], data that are crucial to the quantification of key aerodynamic parameters and, consequently, the updated maximum take off mass and operational requirements.
In the case of high-speed aircraft, it is convenient to adopt simplified models available in the literature, such as the Raymer and Torenbeek methods. Both are particularly suitable in the case of general configurations characterised by a clear distinction between the fuselage and the delta wing, thus being able to evaluate the intrinsic aerodynamic coefficients of each individual part (fuselage, wing, tail, nacelles, air intakes, ...) and estimate the lift coefficient rather accurately. However, the latter appears less precise in predicting the drag coefficient, which seems to be overestimated as the angle of incidence increases.
Based on these assumptions, the Raymer aerodynamic model is considered, and suitably corrected, by sources in the literature [8], in order to best describe the aerodynamic behaviour of any aircraft with a similar configuration.
In particular, it aims to preliminarily describe the aerodynamic characteristics of the aircraft, including subsonic (M≤0.8), transonic and supersonic (M≥1.2) motion.

5.1 Lift Coefficient

The lift coefficient is expressed as a function of the angle of incidence, where the slope of the curve is evaluated differently depending on the flight regime.

$$Subsonic \rightarrow C_L = C_{L_\alpha}\alpha = \frac{4.5\pi AR}{2+\sqrt{4+\frac{AR^2\beta^2}{\eta^2}\left(1+\frac{\tan^2\Lambda_{max}}{\beta^2}\right)}}\left(\frac{S_{exp}}{S_{ref}}\right)(F)\alpha$$

[1]These terms are specified in Chapter 7.

Where the parameters involved in the formulation are:

- AR, the wing aspect ratio;
- $\beta = \sqrt{1 - M^2}$;
- η, the airfoil efficiency;
- Λ_{max}, the wing sweep at the chord location where the airfoil is thickest;
- S_{exp}, the wing reference area less the part covered by fuselage;
- S_{ref}, the wing reference area;
- F, the fuselage lift factor.

$$Supersonic \rightarrow C_L = C_{L_\alpha} = \frac{4}{\beta}\alpha$$

Where the parameters involved in the formulation are:

- $\beta = \sqrt{M^2 - 1}$;

In the transonic regime, there are no methods for estimating the slope of the lift curve. Therefore, the calculated subsonic and supersonic values are first plotted, as a function of Mach number, and then interpolated to determine a result.
In addition, the maximum lift coefficient must be defined punctually, as it cannot be calculated from the routine.

5.2 Drag Coefficient

The drag coefficient is instead expressed as the sum of the parasitic drag C_{D_0} and the induced drag C_{D_i}, where the former is dictated by the contribution of the coefficient of *Skin Friction Drag*, *Miscellaneous Drag* and, possibly, *Wave Drag*.

$$Subsonic \rightarrow C_{D_0} = \frac{\sum(C_{f_c} FF_c Q_c S_{wet_c})}{S_{ref}}(1 + 0.02) + C_{D_{misc}}$$

Where the parameters involved in the formulation are:

- C_{f_c}, the skin friction coefficient;
- FF_c, the component form factor;
- Q_c, the interference effect factor;
- S_{wet_c}, the aircraft wetted surface;

- S_{ref}, the wing reference area;
- $C_{D_{misc}}$, the additional drag component to account for various miscellaneous objects sticking out into the flow.

$$Supersonic \rightarrow C_{D_0} = \frac{\sum(C_{f_c} FF_c Q_c S_{wet_c})}{S_{ref}}(1+0.02) + C_{D_{misc}} + C_{D_{wv}}$$

Where the parameters involved in the formulation are:

- C_{f_c}, the skin friction coefficient;
- FF_c, the component form factor;
- Q_c, the interference effect factor;
- S_{wet_c}, the aircraft wetted surface;
- S_{ref}, the wing reference area;
- $C_{D_{misc}}$, the additional drag component to account for various miscellaneous objects sticking out into the flow;
- $C_{D_{wv}}$, the extra drag at supersonic speeds and accounts for the pressure drag due to shock formation; this new term, supersonic, will often be greater than all of the other drugs put together.

$$Subsonic \rightarrow C_{D_i} = KC_L^2 = \frac{1}{\pi ARe} C_L^2$$

Where the parameters involved in the formulation are:

- AR, the wing aspect ratio;
- e, the Oswald efficiency factor, that accounts for the extra drag due to the non-elliptical lift distribution.

$$Supersonic \rightarrow C_{D_i} = KC_L^2 = 1.5 \frac{AR(M^2-1)\cos\Lambda_{LE}}{4AR + \sqrt{M^2-1} - 1} C_L^2$$

Where the parameters involved in the formulation are:

- AR, the wing aspect ratio;
- Λ_{LE}, the leading edge sweep.

In the transonic regime, there are no methods for estimating the slope of the drag curve. Therefore, the calculated subsonic and supersonic values are first plotted, as a function of Mach number, and then interpolated to determine a result.

Chapter 6

Iterative Cycle

One of the main design values is the take off mass, defined as the sum of the mass of pilots and attendants, payload, fuel and empty mass.

$$MTO = crew + payload + fuel + OEM \tag{6.1}$$

Under conditions of maximum payload and non-zero range, the take off mass tends to coincide with the maximum take off mass, a quantity that is already statistically quantified, but can be further refined, through the implementation of an iterative cycle suggested by the Raymer method [20].

In fact, by reworking Equation 6.1, it is possible to obtain a numerically solvable expression of the maximum take off mass, in which all terms are known[1], except for the fuel and empty mass fractions, which can be determined through considerations and estimates.

$$MTOM = \frac{crew + payload}{1 - \frac{fuel}{MTOM} - \frac{OEM}{MTOM}} \tag{6.2}$$

6.1 Fuel Mass Fraction

The fuel mass fraction is related to the mission profile, specific fuel consumption and aerodynamics, and can be formulated as:

$$\frac{fuel}{MTOM} = 1 - \frac{m_{end_{10}}}{MTOM}$$

Where $\frac{m_{end_{10}}}{MTOM}$ denotes the ratio of the final mass to the initial mass, associated with the trajectory described in the previous chapter[2] and determined by multiplying the mass fractions, relative to each segment and generated by fuel consumption.

$$\frac{m_{end_{10}}}{MTOM} = \frac{m_{end_1}}{MTOM} \frac{m_{end_2}}{m_{end_1}} \frac{m_{end_3}}{m_{end_2}} \frac{m_{end_4}}{m_{end_3}} \frac{m_{end_5}}{m_{end_4}} \frac{m_{end_6}}{m_{end_5}} \frac{m_{end_7}}{m_{end_6}} \frac{m_{end_8}}{m_{end_7}} \frac{m_{end_9}}{m_{end_8}} \frac{m_{end_{10}}}{m_{end_9}}$$

[1] $crew$ can be calculated as the product of the 4 crew members and 100 kg, which is the sum of the mass of each individual and their luggage.

[2] Compared to the route described in Chapter 4, the *second segment* is introduced, the difference between supersonic and subsonic descent is neglected, and the descent prior to landing is assumed to be within the holding [20].

In particular, if for the take off, climb, descent and landing phases the values of these contributions can be derived experimentally, evaluating a concept similar to that of the aircraft in question, for the cruise phases it is necessary to refer to the Breguet equation, a function of:

- partial range R, variable according to the phase;
- speed v, equal to the product of the Mach number and the speed of sound at the selected flight altitude;
- specific fuel consumption SFC, constant for simplicity during the trajectory and equal to 4.1e-5 kg/(N*s);
- aerodynamic efficiency E, equal to the ratio between the lift and drag coefficient in the selected flight condition.

Phase	Mass Fraction	Value
Take Off	$m_{end_1}/MTOM$	0.97
Second Segment	m_{end_2}/m_{end_1}	0.999
Subsonic Climb	m_{end_3}/m_{end_2}	0.957
Subsonic Cruise	m_{end_4}/m_{end_3}	$e^{\frac{-R\cdot SFC\cdot g}{v\cdot E}}$=0.924
Supersonic Climb	m_{end_5}/m_{end_4}	0.947
Supersonic Cruise	m_{end_6}/m_{end_5}	$e^{\frac{-R\cdot SFC\cdot g}{v\cdot E}}$=0.668
Descent	m_{end_7}/m_{end_6}	0.931
Climb	m_{end_8}/m_{end_7}	0.985
Holding	m_{end_9}/m_{end_8}	$e^{\frac{-R\cdot SFC\cdot g}{v\cdot E}}$=0.982
Landing	$m_{end_{10}}/m_{end_9}$	0.995

Table 6.1: Mass Fraction Values

6.2 Empty Mass Fraction

The empty mass fraction can be formulated as:

$$\frac{OEM}{MTOM} = a \cdot MTOM^b = 0.97 \cdot MTOM^{-0.06}$$

Where a and b identify two characteristic parameters for the examined aircraft category.

6.3 Maximum Take Off Mass

In possession of all the terms necessary to calculate the maximum take off mass, it is possible to initialise the iterative procedure[3] to solve Equation 6.2 cyclically until a convergence value is reached.
The process tends to converge in 12 iterations to a final solution of 180092.61 kg.

[3]Based on the algorithm coded in Python, the empty mass fraction is calculated initially, but not updated subsequently; only the fuel fraction, and consequently the maximum take off mass, is changed iteratively.

Chapter 7

Matching Chart

The aircraft must be able to meet precise operational and environmental requirements during mission execution, ensuring efficient performance combined with an adequate safety margin.
The purpose of the Matching Chart is to graphically illustrate the various constraints, through the evolution of the T/W ratio as a function of the wing loading W_{kg}/S, in order to delineate a feasible design space and, consequently, an optimal design point, capable of defining a unique and coherent configuration with regard to wing area and propulsive thrust.

7.1 Operational Requirements

Operational requirements are related to mathematical relations inherent to the main mission phases, duly corrected to represent sea level equivalent trends.

Take Off

Take off takes place in the following flight condition:

Mach [-]	Altitude [m]	Angle of Incidence [deg]	Throttle Percentage [%]
0.35	100	20	95

Table 7.1: Take Off Condition

The relationship is expressed as follows:

$$\frac{T}{W} = \frac{1}{\rho C_L l_{TO} \sigma} \frac{W_{kg}}{S}$$

Where the parameters involved in the formulation are:

- $\rho = 1.213\ kg/m^3$, the density at the selected altitude;
- $C_L = 0.8$, the lift coefficient;
- $l_{TO} = 2000\ m$, the maximum take off distance;
- $\sigma = 0.990$, the density ratio.

Second Segment

Second segment takes place in the following flight condition:

Mach [-]	Altitude [m]	Angle of Incidence [deg]	Throttle Percentage [%]
0.4	150	15	95

Table 7.2: Second Segment Condition

The relationship is expressed as follows:

$$\frac{T}{W} = \left(\frac{N_{eng}}{N_{eng}-1}\right)\left(\frac{1}{E} + G_{2nd}\right)\frac{1}{\sigma}$$

Where the parameters involved in the formulation are:

- $N_{eng} = 4$, the engine number;
- $E = 4.972$, the aerodynamic efficiency;
- $G_{2nd} = 4\%$, the second segment climb gradient;
- $\sigma = 0.986$, the density ratio.

Subsonic Climb

Subsonic climb takes place in the following flight condition:

Mach [-]	Altitude [m]	Angle of Incidence [deg]	Throttle Percentage [%]
0.5	3500	10	90

Table 7.3: Subsonic Climb Condition

The relationship is expressed as follows:

$$\frac{T}{W} = \frac{q_\infty C_D}{g\Pi\sigma}\frac{1}{\frac{W_{kg}}{S}} + G_{sub}\frac{1}{\Pi\sigma}$$

Where the parameters involved in the formulation are:

- $q_\infty = 11512\ Pa$, the dynamic pressure;
- $C_D = 0.069$, the drag coefficient;
- $g = 9.81\ m/s^2$, the gravitational acceleration;
- $G_{sub} = 2\%$, the subsonic climb gradient;
- $\Pi = 90\%$, the throttle percentage;
- $\sigma = 0.705$, the density ratio.

Subsonic Cruise

Subsonic cruise takes place in the following flight condition:

Mach [-]	Altitude [m]	Angle of Incidence [deg]	Throttle Percentage [%]
0.8	12000	3	80

Table 7.4: Subsonic Cruise Condition

The relationship is expressed as follows:

$$\frac{T}{W} = \frac{q_\infty C_D}{g\Pi\sigma}\frac{1}{\frac{W_{kg}}{S}}$$

Where the parameters involved in the formulation are:

- $q_\infty = 8690\ Pa$, the dynamic pressure;
- $C_D = 0.012$, the drag coefficient;
- $g = 9.81\ m/s^2$, the gravitational acceleration;
- $\Pi = 80\%$, the throttle percentage;
- $\sigma = 0.254$, the density ratio.

Supersonic Climb

Supersonic climb takes place in the following flight condition:

Mach [-]	Altitude [m]	Angle of Incidence [deg]	Throttle Percentage [%]
0.9	15000	5	1

Table 7.5: Supersonic Climb Condition

The relationship is expressed as follows:

$$\frac{T}{W} = \frac{q_\infty C_D}{g\Pi\sigma}\frac{1}{\frac{W_{kg}}{S}} + G_{sup}\frac{1}{\Pi\sigma}$$

Where the parameters involved in the formulation are:

- $q_\infty = 6867\ Pa$, the dynamic pressure;
- $C_D = 0.028$, the drag coefficient;
- $g = 9.81\ m/s^2$, the gravitational acceleration;
- $G_{sup} = 1\%$, the supersonic climb gradient;
- $\Pi = 1\%$, the throttle percentage;
- $\sigma = 0.158$, the density ratio.

Supersonic Cruise

Supersonic cruise takes place in the following flight condition:

Mach [-]	Altitude [m]	Angle of Incidence [deg]	Throttle Percentage [%]
2	18000	1	75

Table 7.6: Supersonic Cruise Condition

The relationship is expressed as follows:

$$\frac{T}{W} = \frac{q_{\infty} C_D}{g \Pi \sigma} \frac{1}{\frac{W_{kg}}{S}}$$

Where the parameters involved in the formulation are:

- $q_{\infty} = 21182\ Pa$, the dynamic pressure;
- $C_D = 0.006$, the drag coefficient;
- $g = 9.81\ m/s^2$, the gravitational acceleration;
- $\Pi = 75\%$, the throttle percentage;
- $\sigma = 0.099$, the density ratio.

Landing

Landing takes place in the following flight condition:

Mach [-]	Altitude [m]	Angle of Incidence [deg]	Throttle Percentage [%]
0.3	50	3	40

Table 7.7: Landing Condition

The relationship is expressed as follows:

$$\frac{W_{kg}}{S} = k_L C_{L_{max}} l_{LAND} \sigma$$

Where the parameters involved in the formulation are:

- $k_L = 0.149\ kg/m^3$, the Loftin parameter,
- $C_{L_{max}} = 0.8$, the maximum lift coefficient;
- $l_{LAND} = 3500\ m$, the maximum landing field length;
- $\sigma = 0.995$, the density ratio.

7.2 Environmental Requirements

The environmental requirements are related to mathematical relations concerning noise and pollutant emission levels during the LTO cycle.
Analytical expressions can be produced using a statistical approach, based on the use of ICAO noise and emission database [17, 16] and the consideration of only twin-engine, three-engine and four-engine subsonic aircraft, excluding business jets, developed since the 2000s[1].
Based on this range, the equations for the wing loading W_{kg}/S and the T/W ratio respectively are extrapolated as a function of the same variable and then, by solving a linear system, the direct function of T/W with respect to W_{kg}/S is calculated.

Noise

In the case of noise, the independent variable is the difference between the sum of the maximum permissible levels and the 17 dB margin, according to Equation 1.1.

$$(LIMIT_A + LIMIT_F + LIMIT_L) - 17 = 0$$

Consider the entities listed here, where *Margin* is defined by the above expression.

Aircraft	Engine Number	$LIMIT_A$	$LIMIT_F$	$LIMIT_L$	Margin	W_{kg}/S	T/W
A310-200	2	102.7	95.3	99.2	280.2	648	0.3130
A318-100	2	100.2	91.0	96.5	270.7	556	0.3178
A319-100	2	100.6	91.7	96.9	272.2	617	0.3198
A320-200	2	100.6	91.6	96.8	272.0	609	0.3240
A321-200	2	101.3	92.8	97.6	274.7	730	0.3096
A330-200	2	104.4	98.2	101.1	286.7	658	0.2613
A340-200	4	104.9	104.1	101.6	293.6	757	0.2239
A340-300	4	104.8	103.7	101.4	292.9	716	0.2368
A340-500	4	105.0	105.8	102.8	296.6	855	0.2835
A340-600	4	105.0	105.7	102.7	296.4	842	0.3047
A350-900	2	105.0	99.2	101.7	288.9	633	0.2760
A350-1000	2	105.0	99.9	102.1	290.0	681	0.2813
A380-841	4	105.0	106.0	103.0	297.0	680	0.2468
B737-800	2	100.7	91.9	97.0	272.6	634	0.3096
B737-900	2	100.7	91.9	97.0	272.6	634	0.3096
B737-8	2	100.9	92.1	97.2	273.2	651	0.3207
B737-9	2	101.1	92.5	97.4	274.0	695	0.3001
B757-300	2	102.3	94.5	98.7	278.5	673	0.3122
B777-F	2	105.0	100.4	102.5	290.9	796	0.3013
B787-8	2	104.3	98.0	100.9	286.2	605	0.2880
B787-9	2	104.6	98.5	101.3	287.4	662	0.2844
B787-10	2	104.7	98.6	101.3	287.6	674	0.2809

Table 7.8: ICAO Aircraft Noise Database

[1]The database therefore consists of a set of civil aircraft, albeit subsonic, characterised by the latest and most modern propulsion systems and, therefore, the most efficient and least polluting.

It is noted that as the size of the aircraft increases in terms of wing area, weight and thrust, the regulations impose less and less stringent requirements (Figure 7.1).

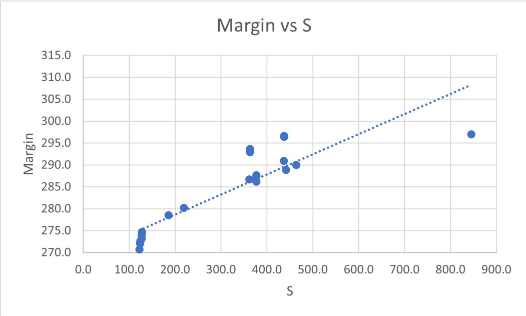

(a) Margin vs S

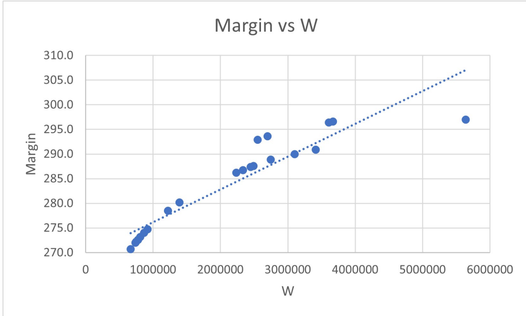

(b) Margin vs W

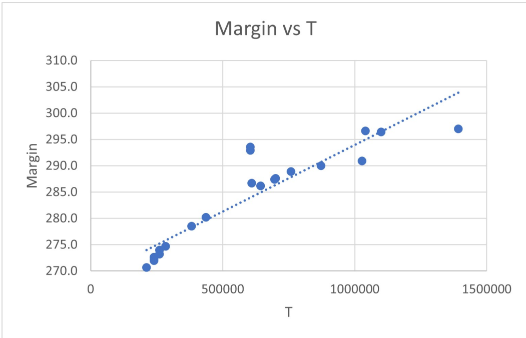

(c) Margin vs T

Figure 7.1: Noise Level

In addition, the negative slope of the final trend (Figure 7.2 (c)) shows that, as W_{kg}/S increases, the T/W ratio must necessarily decrease to comply with the environmental requirement.

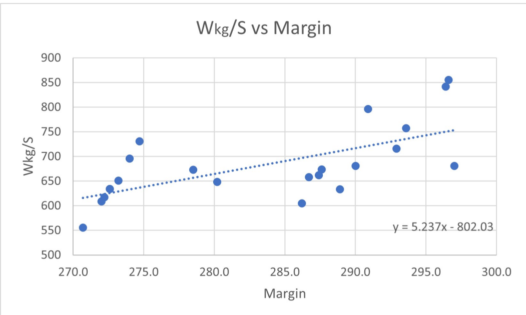

(a) W_{kg}/S vs Margin

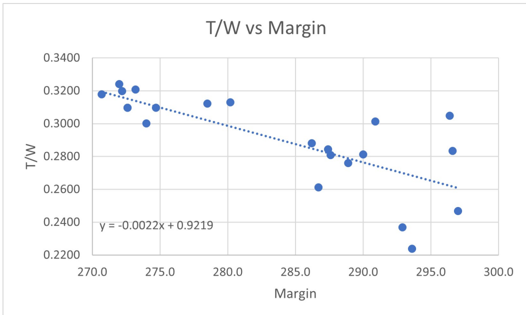

(b) T/W vs Margin

(c) T/W vs W_{kg}/S

Figure 7.2: Noise Level

Pollutant Emissions

In the case of pollutant emissions, the independent variable is the sum of the maximum release levels of carbon monoxide, nitrogen oxides and unburned hydrocarbons, according to Equations 1.2, 1.3 and 1.4.

$$CO + NO_x + HC = \left[4550(\pi_\infty)^{-1.03}\right] + \left[36 + 2.42\pi_\infty\right] + \left[140(0.92)^{\pi_\infty}\right]$$

Consider the entities listed here, where *Cumulative* is defined by the above expression multiplied by the engine number.

Aircraft	Engine Number	π_∞	CO	NO_X	HC	Cumulative	W_{kg}/S	T/W
A310-200	2	28.0	147.04	103.76	13.56	528.72	648	0.3130
A318-100	2	28.0	147.04	103.76	13.56	528.72	556	0.3178
A319-100	2	27.3	150.93	102.07	14.37	534.73	617	0.3198
A320-200	2	24.6	167.73	95.63	17.94	562.61	609	0.3240
A321-200	2	31.3	131.10	111.75	10.30	506.28	730	0.3096
A330-200	2	33.1	123.84	116.05	8.88	497.54	658	0.2613
A340-200	4	31.2	131.75	111.38	10.43	1014.23	757	0.2239
A340-300	4	31.2	131.75	111.38	10.43	1014.23	716	0.2368
A340-500	4	35.2	116.20	121.16	7.44	979.21	855	0.2835
A340-600	4	36.7	111.25	124.84	6.56	970.57	842	0.3047
A350-900	2	41.1	99.05	135.44	4.55	478.08	633	0.2760
A350-1000	2	48.6	83.38	153.54	2.44	478.71	681	0.2813
A380-841	4	39.0	104.61	130.31	5.43	961.38	680	0.2468
B737-800	2	25.8	160.10	98.39	16.31	549.60	634	0.3096
B737-900	2	25.6	161.26	97.95	16.56	551.54	634	0.3096
B737-8	2	39.9	102.04	132.61	5.02	479.34	651	0.3207
B737-9	2	41.5	98.04	136.43	4.40	477.75	695	0.3001
B757-300	2	27.9	147.37	103.61	13.63	529.21	673	0.3122
B777-F	2	42.2	96.28	138.22	4.14	477.26	796	0.3013
B787-8	2	41.9	97.08	137.40	4.25	477.47	605	0.2880
B787-9	2	42.2	96.37	138.12	4.15	477.29	662	0.2844
B787-10	2	47.5	85.31	150.95	2.67	477.86	674	0.2809

Table 7.9: ICAO Aircraft Emission Database

It is noted that as the size of the aircraft increases in terms of wing area, weight and thrust, the regulations impose less and less stringent requirements (Figure 7.3).

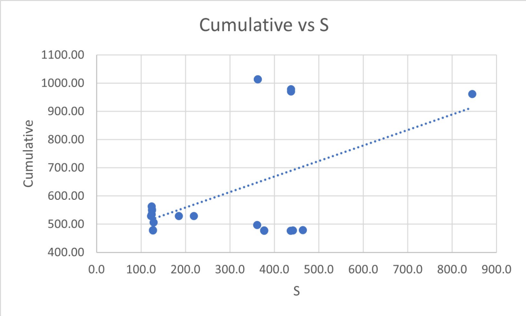

(a) Cumulative vs S

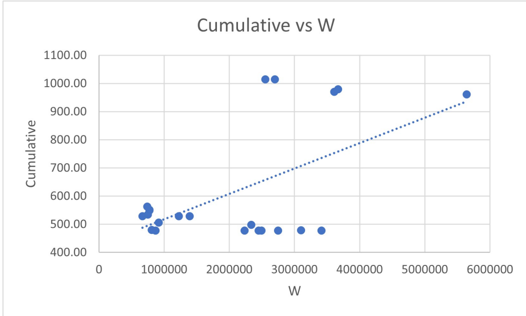

(b) Cumulative vs W

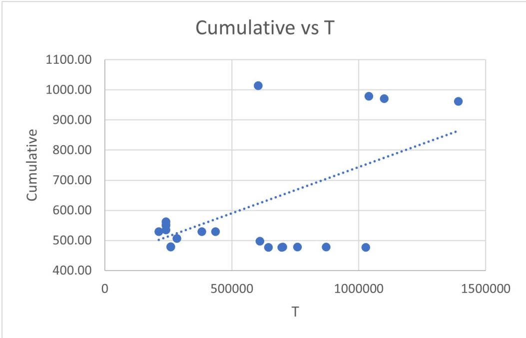

(c) Cumulative vs T

Figure 7.3: Emission Level

In addition, the negative slope of the final trend (Figure 7.4 (c)) shows that, as W_{kg}/S increases, the T/W ratio must necessarily decrease to comply with the environmental requirement.

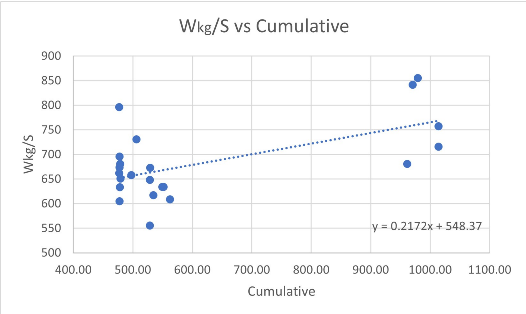

(a) W_{kg}/S vs Cumulative

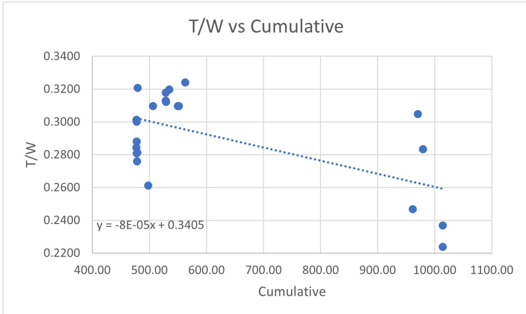

(b) T/S vs Cumulative

(c) T/W vs W_{kg}/S

Figure 7.4: Emission Level

7.3 Design Point

The design space can be identified at the part of the graph marked by the T/W ratio, above the most stringent operational requirement and below the most critical environmental requirement. From the point of view of an environmentally sustainable aircraft, assuming an engine without afterburner[2], the design point is located at the intersection between the operational constraints of supersonic cruise and landing and the environmental constraint of pollutant emissions, indicated by the point $W_{kg}/S = 417.45\ kg/m^2$ - $T/W = 0.39$ (⋆ in Figure 7.5 (b)).
In this way, it is possible to obtain the updated values of the wing area and propulsive thrust.

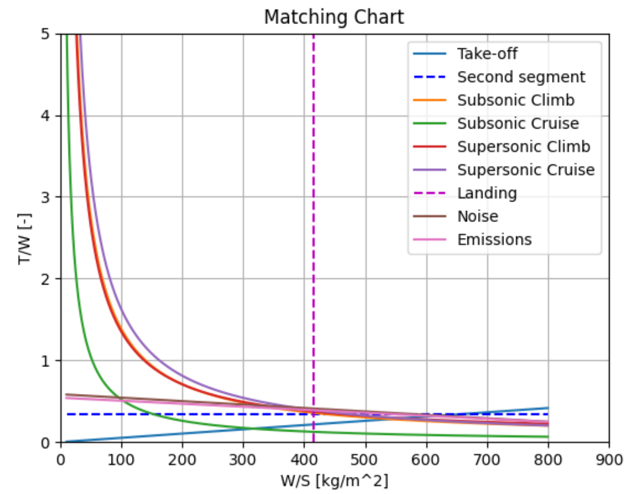

(a) Matching Chart

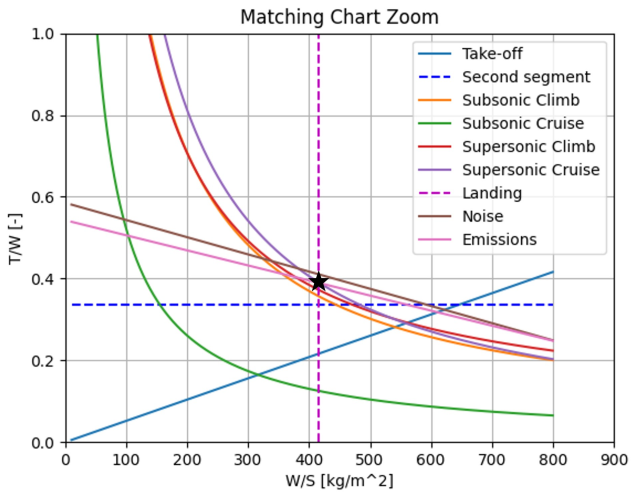

(b) Matching Chart Zoom

Figure 7.5: Design Point

$$\begin{cases} \frac{W_{kg}}{S} & = 417.45\ \frac{kg}{m^2} \\ \frac{T}{W} & = 0.39 \end{cases} \Rightarrow \begin{cases} S = (\frac{W_{kg}}{S})^{-1} \cdot MTOM & = 431.41\ m^2 \\ T = \frac{T}{W} \cdot MTOM \cdot g & = 689.02\ kN \end{cases}$$

[2]In the case of an afterburner engine, the supersonic cruise operational requirement would be described by a further upward shift.

In the case of the *Aérospatiale-BAC Concorde*, the design point ($W_{kg}/S = 516.59$ kg/m^2 - $T/W = 0.37$ ($\star$ in Figure 7.6)) does not meet the environmental requirements compared to the aircraft under analysis.
However, it should be emphasised that the Matching Chart is hardly capable of correlating different engine types; therefore, a more rigorous comparison could only be made with the same level of engine technology. In fact, the *Aérospatiale-BAC Concorde* is presented with an outdated turbojet engine with an afterburner, whereas the aircraft under discussion has an innovative turbofan without an afterburner, a condition that necessarily guarantees lower noise, consumption and emissions.
Ultimately, as these aircraft are designed with completely different engines, it is complex to make a meaningful comparison. This Matching Chart is therefore only a valid comparison tool in view of future configurations related to advanced solutions.

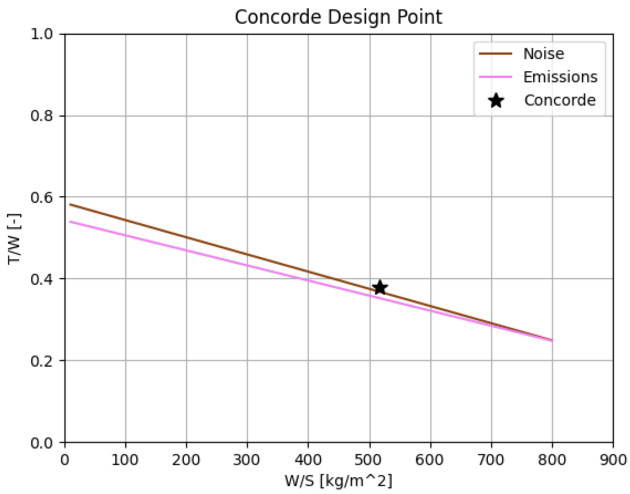

Figure 7.6: Concorde Design Point

Chapter 8

Updated Sizing

The final sizing consists of a refinement of the initial configuration, by further application of the statistical approach (Figure 3.2), albeit from the updated maximum take off mass, thus resulting in a variation of only the geometric characteristics of the wing and tail, being dependent on it.

OEM [kg]	Payload [kg]	Crew [kg]	Fuel [kg]	MTOM [kg]	Thrust [kN]	SFC [kg/(N*s)]
75215.95	12000	400	92476.65	180092.61	689.02	4.2e-05

Table 8.1: Performance Sizing

Fuselage Length [m]	Fuselage Width [m]	Fuselage Height [m]	Aircraft Height [m]
58.92	2.81	2.94	10.95

Table 8.2: Fuselage Sizing

Area [m^2]	Span [m]	AR [-]	Root Chord [m]	Tip Chord [m]	MAC [m]	λ [-]	Mean Sweep Angle [deg]
431.41	28.6	1.6	34.08	2.27	22.81	0.07	62.44

Table 8.3: Wing Sizing

Area [m^2]	Span [m]	AR [-]	Root Chord [m]	Tip Chord [m]	MAC [m]	λ [-]	Mean Sweep Angle [deg]
61.38	5.1	0.42	11.49	2.88	8.05	0.25	60.51

Table 8.4: Tail Sizing

In which the performance parameters and wing area are derived from the results calculated in the previous chapters.

Geometrically, the layout does not differ too much from what has already been achieved, resulting in a distribution of cross-sectional areas that still deviates from the *Sears-Haack* trend.

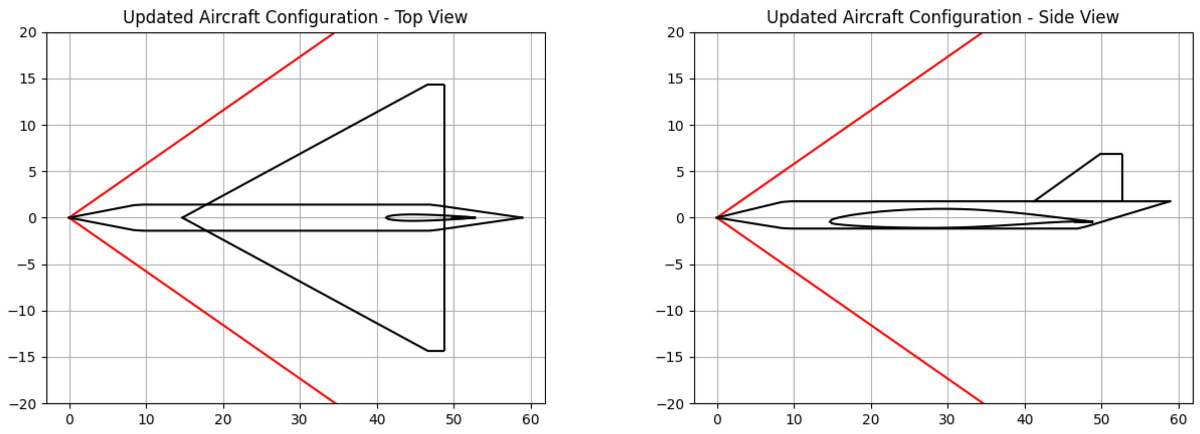

(a) Top View (b) Side View

Figure 8.1: Updated Configuration

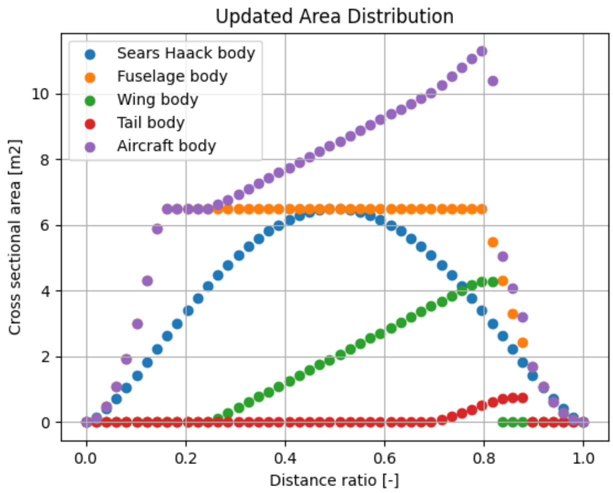

Figure 8.2: Updated Area Distribution

In this regard, the proposed concept requires a refinement of the geometry using the rule of areas, thus ensuring a gradual development of the transverse surfaces along the aircraft axis and a reduction of the fuselage section in the wing junction area, with the aim of minimising wave resistance and consequently optimising performance.

For the formalisation and subsequent realisation of the aircraft, it will therefore be essential to make use of the preliminary and detailed design phases, in order to re-evaluate the entities involved, improve the structural model and arrive at an ideal final solution[1].

However, this approximate configuration still needs to be defined in terms of profile and engine.

[1]These aspects are beyond the scope of this study.

8.1 Profile

The wing and tail profiles are represented by *NACA 65-206* and *NACA 0006* respectively.
The first identifies a supercritical 6-digit profile characterised by 1.1% maximum curvature, located at 50% of the chord, and 6% maximum thickness, located at 40% of the chord. This is the same typology adopted by the *Aérospatiale-BAC Concorde*, which can delay as much as possible the occurrence of the transition from laminar to turbulent flow, thus reducing the negative compressible effects.

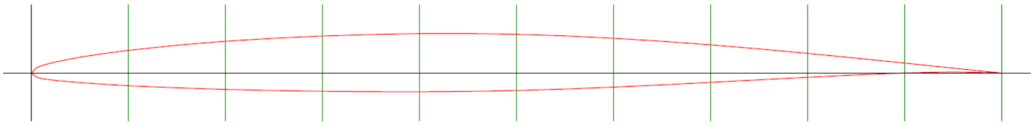

(a) Wing Profile

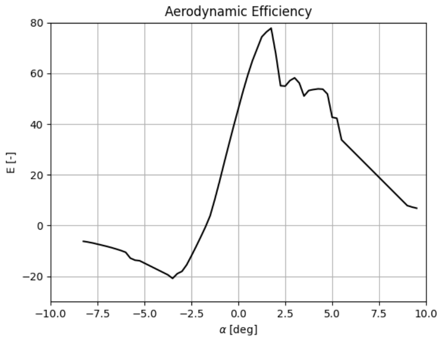

(b) Aerodynamic Efficiency

Figure 8.3: NACA 65-206

The second, on the other hand, identifies a symmetrical 4-digit profile characterised by 6% maximum thickness, located at 30% of the chord, which can confer similar aerodynamic behaviour for both positive and negative incidence angles.

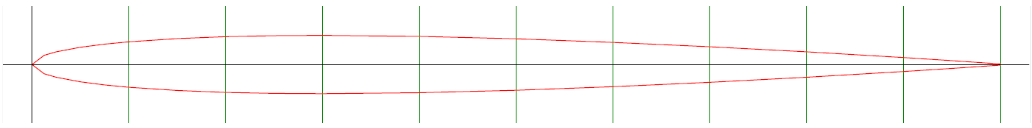

(a) Tail Profile

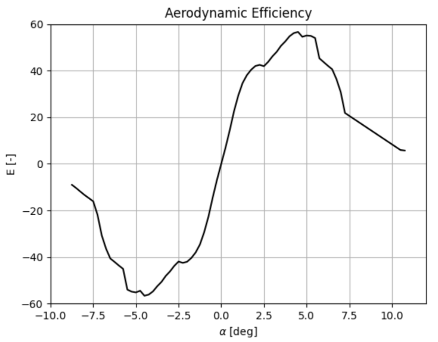

(b) Aerodynamic Efficiency

Figure 8.4: NACA 0006

Specifically, the delta wing is equipped with a twisting of the different profiles along the span, containing the onset of aerodynamic stall phenomena, as well as a double sweep angle, useful to perceive a lower Mach value and limit the generation of shock waves, albeit with a reduction in lift. It also has a negative dihedral angle, which improves lateral maneuverability, especially in certain specific flight conditions.

8.2 Engine

The engine is identified by an advanced and innovative solution, developed specifically for the aircraft in question.
Considering that existing supersonic engines are equipped on fighter aircraft, neither able to reduce fuel consumption nor ensure the reliability required for commercial aviation, the best alternative is to devise a turbofan architecture capable of delivering 173 kN of thrust without an afterburner, sustaining supersonic cruise at Mach 2, burning only sustainable aviation fuel and optimising specific consumption[2] with respect to previously established. In this way, it is possible to generate the required total thrust of 689.02 kN through four thrusters, increased by a certain safety margin, limiting the environmental impact.
The design features an asymmetric supersonic intake, combined with a passively cooled, high-pressure turbine and a low-noise, variable-geometry exhaust nozzle to generate the required propulsive force and meet both operational and environmental requirements.

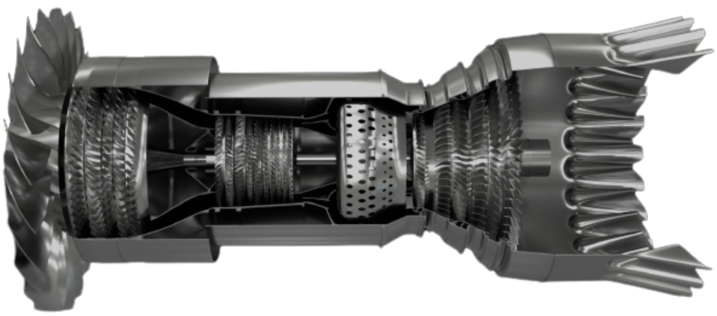

Figure 8.5: Possible Engine Layout

8.3 Sonic Boom

The resulting configuration must also be evaluated in terms of the sonic boom generated during the cruise condition. Although this aspect is not dealt within the Python routines, an article in the literature proposes numerical reference values in this regard, based on an aircraft with almost the same performance and geometric characteristics as the one presented in the following discussion.

[2]The statistically determined value of the SFC is excessively high.

The sonic boom identifies a crucial aspect of supersonic aircraft design, as its impact on the perceived noise levels on the ground is critical for safety and air traffic regulation. Specifically, "the parameters that most influence the level of sonic boom intensity are related to the aircraft's flight altitude, Mach number at cruise, wind, and weight" [9]. The phenomenon occurs during flight and is caused by a system of shock waves that can propagate to the ground through the atmosphere. This propagation can culminate in a significant increase in noise levels, raising concerns in terms of annoyance to the population and consequently leading to restrictions on overflying continental areas.

Although ICAO standards do not currently explicitly regulate the sonic boom, which therefore cannot be directly integrated within the Matching Chart, it is essential to consider its analysis from the initial design stages of a high-speed aircraft. To this end, the literature proposes the *Carlson Method*, a simplified approach derived from studies based on the theory of linearised supersonic flow. By focusing on physical, environmental and geometric characteristics, it can provide reliable estimates without requiring a large amount of data.

The *Carlson Method* is applicable to all supersonic aircraft under various conditions, including stationary flight and slight climb/descent up to an altitude of about 76 km. However, it is important to note some limitations: for example, the model takes into account, as variables, a windless atmosphere and only N-waves. The latter consists of a compression, followed by a linear expansion to a pressure below the ambient pressure, and then a second peak, which is used to restore the pressure value to zero.

In a specific investigation concerning approximately the same aircraft, cruising at Mach 2 and powered by biofuel, the methodology was evaluated against a high-fidelity study consisting of two phases: the use of a CFD (*Computational Fluid Dynamics*) simulation, capable of modelling shock waves in the *near field*, and the application of a tool to simulate their propagation towards the ground, through the atmosphere (*far field*).

The research identified aerodynamic overpressure values, responsible for the sonic boom, in different radial directions around the aircraft geometry. These turned out to be slightly higher than those provided by the high-fidelity study, confirming the *Carlson Method*'s ability to remain conservative by about 5%-10%. This can be inferred from the results shown in Table 8.5.

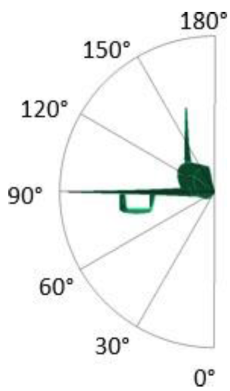

Figure 8.6: Radial Directions

Radial Direction [deg]	Carlson Method [Pa]	High Fidelity Study [Pa]
0	58.2	57.04
10	57.53	55.78
20	53.91	50.39
30	48.77	43.61
40	42.23	40.97
50	35.03	32.26

Table 8.5: Aerodynamic Overpressure Values

Therefore, the results of the in-depth study indicated a good correlation between the two methodologies, with differences within acceptable limits for the conceptual design phase. This suggests that the *Carlson Method* can be considered a valid tool for preliminary sonic boom estimation, offering a balance between accuracy and practicality in the early design stages [9].

Chapter 9

Biofuel

In the context of the supersonic aircraft conceptual design, the imperative is to explore innovative options that can converge on an efficient and environmentally friendly aviation solution.
In this regard, the relevance of biofuel emerges as a catalyst in the transformation of the aviation sector towards ecological sustainability. It can contribute significantly to the reduction of CO_2 emissions, without substantially altering the aircraft's propulsion system, unlike CO, NO_x and HC emissions, which have a direct impact on design.
Biofuel represents a particular type of SAF (*Sustainable Aviation Fuel*) similar in many aspects to fossil fuel, being liquid at standard temperature and pressure, with high energy density and the same hydrocarbon content, but with the peculiarity of coming from sustainable and renewable sources, such as waste biomass (wheat, maize, beet, sugar cane), vegetable oils, animal fats and municipal solid waste. This enables a reduction in greenhouse gas emissions, over its entire life cycle, of up to 90% compared to conventional fuel, allowing for a systemically smooth transition.

9.1 CO2 Emissions

A biofuel must meet specific sustainability criteria in order to be considered suitable.
According to ICAO standards, it is essential that it ensures a reduction in greenhouse gas emissions of at least 10% compared to fossil fuel, related to the value of 89 gCO_2/MJ (expressed in grams of CO_2 per MJ of propellant burned).
An internationally adopted approach to quantify carbon dioxide release is based on the consideration of both LCA (*Life Cycle Assessment*) emissions, associated with the entire life cycle of the product, and ILUC (*Induced Land Use Change*) emissions, associated with induced land use change.
The former include the phases of:

- cultivation, harvesting and processing of raw material;
- transport of raw material from farms to conversion plants;
- conversion of raw material into fuel;
- transport of fuel from production plants to final use sites;

- combustion of the fuel.

The latter consider the demand for additional land due to:

- start-up of new alternative fuel production (direct land use change);
- moving crops or animals for which the land was previously used (indirect land use change).

The variety of possible raw materials and conversion technologies now results in a multitude of certified routes for use. These include[1]:

Conversion Process	Abbreviation	Possible Feedstocks	Maximum Blend Ratio
Fischer-Tropsch hydroprocessed synthesized paraffinic kerosene	FT	Coal, natural gas, biomass	50%
Synthesized paraffinic kerosene from hydroprocessed esters and fatty acids	HEFA	Bio-oils, animal fat, recycled oils	50%
Synthesized iso-paraffins from hydroprocessed fermented sugars	SIP	Biomass used for sugar production	10%
Alcohol to jet synthetic paraffinic kerosene	ATJ	Biomass from ethanol, isobutanol or isobuthene	50%

Table 9.1: Approved Conversion Processes

Raw materials[2] can be of a different nature.

- Main products (M): represent the result of a production process, show significant economic value and elastic supply (there is a causal link between raw material prices and the quantity of raw materials produced) and include emissions from the cultivation of raw materials.
- Co-products (C): represent the result of a production process, show significant economic value and elastic supply (there is a causal link between raw material prices and the quantity of raw materials produced) and include emissions from the cultivation of raw materials.
- Residues (R): identify secondary materials from agriculture, aquaculture, fisheries, forestry or processing, have little economic value and inelastic supply and do not include emissions from the cultivation of raw materials.
- Wastes (W): identify secondary, partially biogenic and fossil materials, which the holder discards, have no economic value and an inelastic supply and do not include emissions from the cultivation of raw materials.
- By-products (B): identify secondary materials, have an inelastic economic value and supply and do not include emissions from the cultivation of raw materials.

The LCA emissions can be determined as:

$$LCA\ Emissions = e_{fe\_c} + e_{fe\_hc} + e_{fe\_p} + e_{fe\_t} + e_{fefu\_p} + e_{fe\_t} + e_{fu\_c}$$

Where the parameters involved in the formulation describe:

[1]Blending is necessary because certain components of traditional fuel can cause seals to expand in older engines, thus preventing propellant leaks.

[2]The ILUC is only applicable to crops and not to commodity classes R, W and B.

- e_{fe_c}, raw material cultivation;
- e_{fe_hc}, raw material harvesting;
- e_{fe_p}, raw material processing;
- e_{fe_t}, raw material transport;
- e_{fefu_p}, conversion of raw material into fuel;
- e_{fe_t}, fuel transport;
- e_{fu_c}, fuel combustion[3].

Through the application of the expression, the impact of each process along the supply chain can be measured (Figure 9.1).

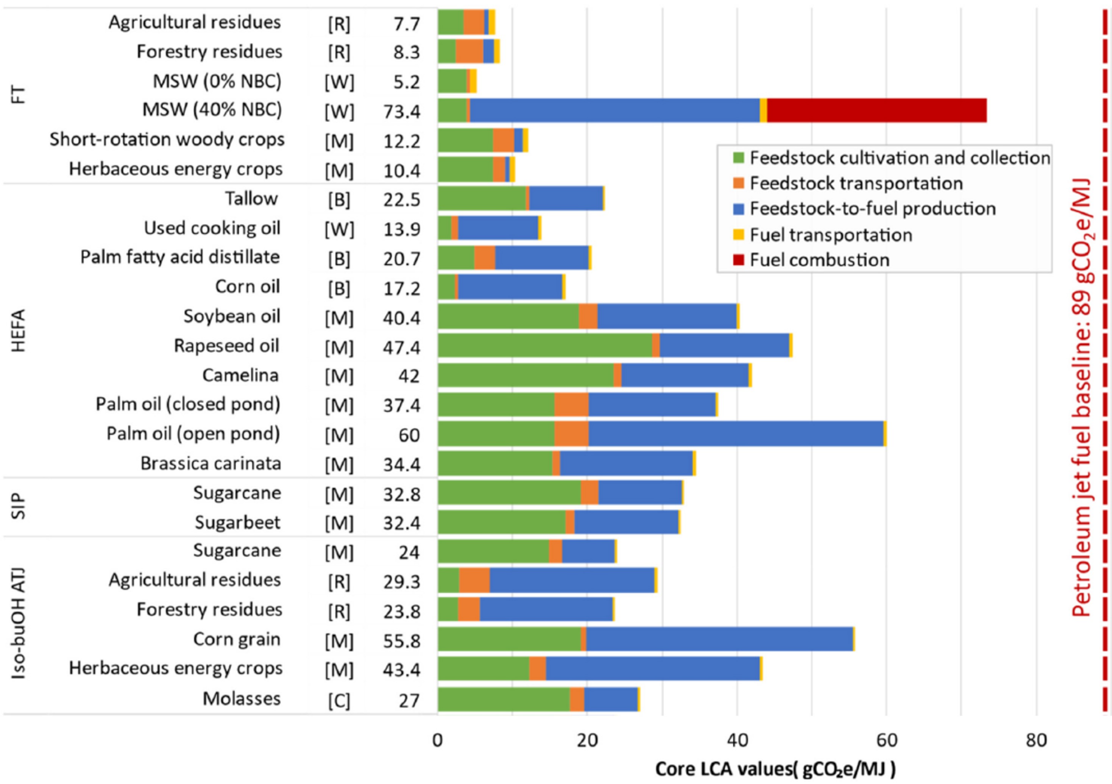

Figure 9.1: LCA Emissions

From which it emerges that:

- main products (M) or co-products (C) determine higher cultivation and harvesting emissions compared to other raw material classes (R, W, B), as the latter are not allocated cultivation emissions;

[3]For fuels derived from biomass, it is assumed that CO_2 emissions from combustion are offset by the absorption of carbon by the biomass through photosynthesis. This occurs during its growth and results in a zero e_{fu_c} contribution, representing an important advantage over conventional fuels.

- different technologies bring a different impact during the conversion from raw material into fuel (e_{fefu_p}) (blue bars in the Figure).
- The FT MSW pathway shows non-zero fuel combustion emissions, due to the 40% non-biogenic carbon composition of the raw material (red bar in the Figure).

The ILUC emissions, on the other hand, can be estimated through appropriate economic models, based on raw material and production place, and directly summarised within the ICAO document [14].

Process	Fuel Feedstock	LCA [gCO_2/MJ]	ILUC [gCO_2/MJ]
FT	Agricultural residues	7.7	0
	Forestry residues	8.3	0
	MSW (0% NBC)	5.2	0
	MSW (40% NBC)	73.4	0
	Short-rotation woody crops	12.2	8.6
	Herbaceous energy crops	10.4	-12.6
HEFA	Tallow	22.5	0
	Used cooking oil	13.9	0
	Palm fatty acid distillate	20.7	0
	Corn oil	17.2	0
	Soybean oil	40.4	25.8
	Rapeseed oil	47.4	26
	Camelina	42	-13.4
	Palm oil (closed pond)	37.4	39.1
	Palm oil (open pond)	60	39.1
	Brassica carinata	34.4	-12.7
SIP	Sugarcane	32.8	11.1
	Sugarbeet	32.4	11.2
Iso-buOH ATJ	Sugarcane	24	9.1
	Agricultural residues	29.3	0
	Forestry residues	23.8	0
	Corn grain	55.8	29.7
	Herbaceous energy crops	43.4	-23.6
	Molasses	27	9.1

Table 9.2: Emission Contributions

Therefore, from the sum of the LCA and ILUL emission contributions, it is possible to compare the result obtained with the reference value of 89 gCO_2/MJ of fossil fuel, in order to calculate a percentage reduction which, when multiplied by the carbon intensity of 3.16 $kgCO_2/kgJetA$ of conventional fuel, allows the carbon intensity of biofuel and, consequently, the net emission reductions to be calculated. This is expressed by Equations 9.1 and 9.2 and summarised in Table 9.3:

$$Carbon\ Intensity = \frac{LCA\ Emissions\ +\ ILUC\ Emissions}{89} \cdot 3.16 \tag{9.1}$$

$$Net\ Emission\ Reduction = \left(1 - \frac{Carbon\ Intensity}{3.16}\right) \cdot 100 \tag{9.2}$$

Process	Fuel Feedstock	Carbon Intensity [$kgCO_2/kgBio$]	Net Emission Reduction [%]
FT	Agricultural residues	0.27	91.35
	Forestry residues	0.29	90.67
	MSW (0% NBC)	0.18	94.16
	MSW (40% NBC)	2.61	17.53
	Short-rotation woody crops	0.74	76.63
	Herbaceous energy crops	-0.08	102.47
HEFA	Tallow	0.80	74.72
	Used cooking oil	0.49	84.38
	Palm fatty acid distillate	0.73	76.74
	Corn oil	0.61	80.67
	Soybean oil	2.35	25.62
	Rapeseed oil	2.61	17.53
	Camelina	1.02	67.87
	Palm (closed pond)	2.72	14.04
	Palm (open pond)	3.52	-11.35
	Brassica carinata	0.77	75.62
SIP	Sugarcane	1.56	50.67
	Sugarbeet	1.55	51.01
Iso-buOH ATJ	Sugarcane	1.18	62.81
	Agricultural residues	1.04	67.08
	Forestry residues	0.85	73.26
	Corn grain	3.04	3.93
	Herbaceous energy crops	0.70	77.75
	Molasses	1.28	59.44

Table 9.3: Net Emission Reductions

9.2 Costs

A biofuel is typically more expensive than a traditional petroleum-based fuel.
In fact, it requires more complex processing to be used as a *drop-in* fuel and to meet the usual operational specifications. At present, high prices make its use unattractive for airlines, as it could lead to an increase in overall operating costs.

According to a study carried out in 2019, the minimum viable value of sustainable propellants always exceeds that of fossil fuels, regardless of the raw material and conversion process, emphasising the need for political support in order for the green alternative to compete with the traditional one.

Specifically, HEFA is the cheapest source of AJF (*Alternative Jet Fuels*), costing between €0.88 and €1.09 per litre, depending on the raw material used. It is therefore the incidence of the latter that determines "approximately half of the (...) production costs for the HEFA fuels" [18], with a value between €400 and €650 per tonne. The survey thus illustrates how, without significant changes in vegetable oil prices, the value of these fuels is unlikely to decrease, due to the high expenses in the acquisition process.

In second place in terms of economy is FT, especially for municipal solid waste propellants, "with a range of €1.34 to €1.87 per liter" [18]. However, the primary costs related to conversion come from a company's upfront investment and are therefore more uncertain than those of HEFA.
On the other hand, the data associated with ATJ show that the initial substances identified with waste biomass "are approximately 40% more expensive to convert into fuel" [18]. A possible cause could be attributable to current raw material and energy costs in addition to conversion costs.
Finally, the production levels of SIP are correlated to the investments needed for sugar conversion, "in which large amounts of a relatively expensive feedstock are converted into" chemical compounds "at low yields" [18]. On the contrary, ATJ, when using sugar cane, proposes higher efficiency through a much more accessible technology. For this reason, SIP process proves to be limiting.

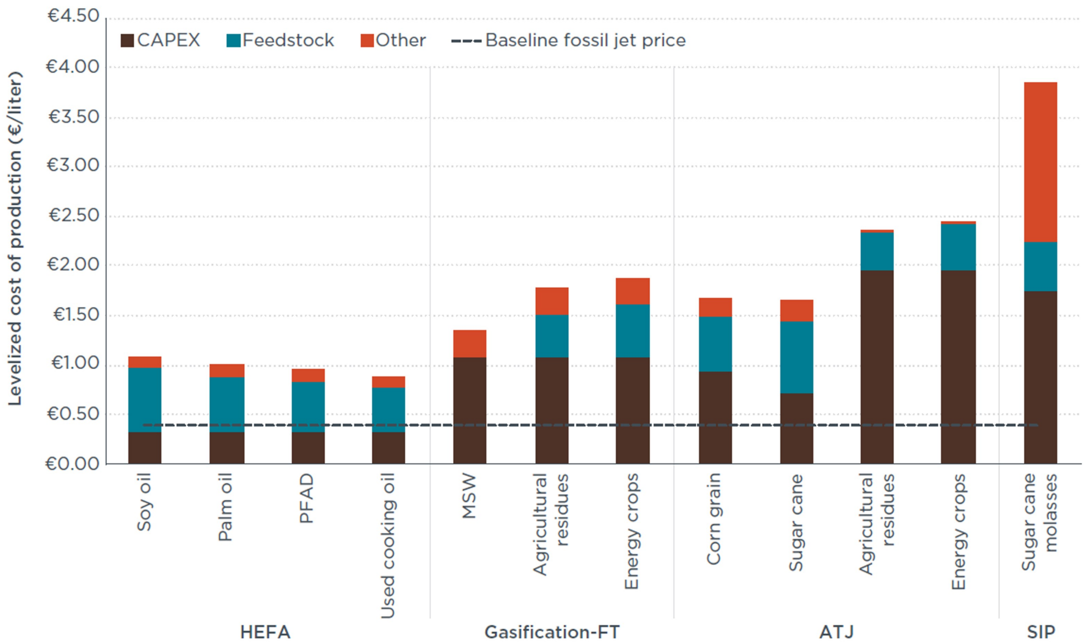

Figure 9.2: Production Costs

9.3 Considerations for the Future

Based on the above-mentioned survey and its results of economic and technological advancement, a series of reflections emerge, useful for evaluating the implementation of the biofuel type, in the short and medium to long term, with relevance to the project developed here.

The most economical fuel is HEFA, as it is easier to market and more common, due to its production through the hydrotreatment of vegetable oils and animal fats. By means of an exothermic reaction, the energy generated initially can be used to reduce the energy costs of the entire process; besides that, the quality of the fuel does not depend on the raw material used. At the aeronautical level, HEFA thus ensures a higher calorific value, faster ignition than Jet A, and less susceptibility

to oxidation. At the same time, despite its many advantages, production costs are unlikely to decrease in the future, as they are linked to high initial resource rates.
It can therefore be seen that this type of sustainable propellant is the most immediate solution for application in the short term, although future challenges must be directed at obtaining low-cost raw materials and refining the process to further reduce the final costs.

By deepening the analysis to identify a medium to long term plan, FT proposes the best solution. It is a technology that is ready to become commercially viable, as it is characterised by a high potential for greenhouse gas emission savings of around 90%, ensuring that municipal solid waste is no longer dumped in landfills, but reused. However, the high capital costs and low application on biomass make FT an unattractive alternative nowadays.
ATJ, due to the abundance of naturally occurring waste material and the resulting emission savings, suggests a viable alternative for a long term plan. Nevertheless, its limited technological advancement requires more effort in the research and development of projects that can support its commercial maturity in the future. In addition, the alcohol used in the process is also an additive for land transport fuels, a condition that could give rise to competitive interests.

Unlike the aforementioned alternative fuels, SIP is not identified as a viable future-oriented proposition due to the expensive initial resources and low yields that can be achieved.

The importance of new challenges related to transport and, consequently, the supply of raw materials becomes clear. The former should be optimally designed, as it is realised that the use of multiple transmission modes in the chain reduces costs and greenhouse gas emissions over the long haul. Supply decisions should also properly evaluate spatial factors, such as the location of raw materials and processing and storage facilities, and temporal factors, such as seasonality, availability and variability of fuel demand. The amount of sustainable propellant produced is still limited, failing to meet the current demand of the aviation industry.
In conclusion, the analyses addressed show the need for policy incentives that ensure a cost parity between innovative methodologies, but also for complementary actions to support technical innovations and limit risks. In this regard, incentives such as grant funding, "could help emerging technologies to scale up production and transition beyond the pioneer plant phase" [18].

Chapter 10

Conclusions

The objectives that this discussion has set itself have been achieved through the use of methods that have already been widely discussed in different studies, but also through variables that have so far only been marginally treated in the literature, despite their fundamental importance.

The first five phases of this research repropose data and analyses typical of the project area, which are therefore relevant but usual in the realisation of such investigations. The Matching Chart elaboration, here conducted by means of not only operational but also environmental constraints, is therefore of crucial importance.

Starting with the iterative cycle, which provides a refinement of the concept of maximum take off mass, defined as the sum of the mass of pilots and attendants, payload, fuel and empty mass, the added value is precisely identified thanks to the Matching Chart. It evaluates the wing loading W_{kg}/S and T/W ratio factors, outlining a feasible design space and optimal design point, through consideration of environmental requirements as well. This allows the wing area S and propulsive thrust T variables to be updated and refined.
This phase was therefore organised starting with the estimation of the operational requirements, moving on to the further observation of the environmental requirements, and finally to the subsequent determination of the design point. The first constraints are related to mathematical relations inherent to the main mission phases, i.e. take off, second segment, subsonic climb and cruise, supersonic climb and cruise, and landing. These must be duly corrected to establish equivalent trends at sea level.
The environmental requirements, on the other hand, are linked to mathematical relations concerning noise and pollutant emissions during the LTO cycle. They are derived using a statistical approach, based on the use of ICAO data, in terms of noise and pollutant emissions, and the evaluation of only twin-engine, three-engine and four-engine subsonic aircraft, excluding business jets, developed since the 2000s. On the basis of this range of aircraft, the equations for the wing loading W_{kg}/S and the T/W ratio respectively are extrapolated as a function of the same variable and then, by solving a linear system, the direct function of T/W with respect to W_{kg}/S is calculated. In the case of noise, the independent variable is obtained as the difference between the sum of the max-

imum permissible levels and the 17 dB margin; in the case of pollutant emissions, it is obtained as the sum of the maximum release levels of carbon monoxide, nitrogen oxides and unburned hydrocarbons. In both cases, it can thus be observed that as the size of the aircraft increases in terms of wing area, weight and thrust, the regulations impose less and less stringent requirements. Furthermore, the negative slope of the final trends shows that, as W_{kg}/S increases, the T/W ratio must necessarily decrease.

For the determination of the design point, the design space was finally considered, identifiable at the part of the graph marked by the T/W ratio, above the most stringent operational requirement and below the most critical environmental requirement. The design point is located at the intersection between the operational constraints of supersonic cruise and landing and the environmental constraint of pollutant emissions, thus arriving at updated values of the wing area and propulsive thrust.

It should be emphasised that the Matching Chart is hardly capable of correlating different engine types; therefore, a possible use and comparison between the aircraft in question and other cases could only be made with the same level of engine technology.

In the seventh stage, the initial geometric characteristics of the wing and tail were updated by further application of the starting statistical approach, as they were dependent on the maximum take off mass, which was refined in the iterative cycle stage. The configuration thus obtained requires a refinement of its geometry through the rule of areas, in order to ensure a gradual development of the transverse surfaces along the aircraft axis and a reduction of the fuselage section in the wing junction area, minimising wave resistance and optimising performance. Therefore, for the aircraft to be effectively formalised and realised, it will be essential to make use of the preliminary and detailed design phase to improve the solution.

For this research, the wing and tail profiles were represented by *NACA 65-206* and *NACA 0006* respectively, the engine by a turbofan architecture, with a thrust of 173 kN without an afterburner developed *ad hoc*, and the sonic boom by a preliminary estimate using the *Carlson Method*, which offers a balance between precision and practicality.

Qualitatively, the study concluded with an investigation of the biofuel properties. It appears to be liquid, at standard temperature and pressure, and comes from sustainable and renewable sources that enable a reduction in greenhouse gas emissions of up to 90% compared to conventional fuel. Among the various types of certified biofuel, the cheapest fuel, in the short term, turned out to be HEFA, as it is easy to market and more common, being derived from the hydrotreatment of vegetable oils and animal fats, despite the high initial resource cost.

On the contrary, in the medium to long term, other alternatives could be evaluated: FT is commercially viable and can reduce greenhouse gas emissions by around 90%, but requires high capital costs; ATJ can instead be obtained from the abundant waste materials found in nature, but is linked to limited technological advancement. The analyses undertaken have therefore shown the need for policy incentives, which can lower burdens, support technical innovations and limit risks.

In addition to the important ecological properties of biofuel, its implementation does not entail any emblematic changes to the aircraft, as it is independent of the design.

This study, with its related methodology, paves the way for the design of more environmentally sustainable supersonic commercial aircraft, offering the opportunity for possible future research.

Bibliography

[1] R. Agosta, D. Bilbija, M. Deutsch, D. Gallant, D. Rose, G. Shreve, D. Smario, and B. Suffredini. The edge supersonic transport. *NTRS - NASA Technical Reports Server*, 1992.

[2] N. E. Antoine and I. M. Kroo. Framework for aircraft conceptual design and environmental performance studies. *AIAA Journal*, 2005.

[3] S. S. Doliente, A. Narayan, J. F. D. Tapia, N. J. Samsatli, Y. Zhao, and S. Samsatli. Bio-aviation fuel: A comprehensive review and analysis of the supply chain components. *Frontiers in Energy Research*, 2020.

[4] J. W. Fenbert, L. P. Ozoroski, K. A. Geiselhart, E. W. Shields, and M. O. McElroy. Concept development of a mach 2.4 high-speed civil transport. *NTRS - NASA Technical Reports Server*, 1999.

[5] D. Ferretto, R. Fusaro, and N. Viola. A conceptual design tool to support high-speed vehicle design. *AIAA Aviation Forum*, 2020.

[6] D. Ferretto, R. Fusaro, and N. Viola. Innovative multiple matching charts approach to support the conceptual design of hypersonic vehicles. *Proceedings of the Institution of Mechanical Engineers, Part G: Journal of Aerospace Engineering*, 2020.

[7] P. D. Gall. Study of an efficient long-range mach 2.7 supersonic transport configuration concept. *NTRS - NASA Technical Reports Server*, 1985.

[8] O. Gori. Simplified models for the preliminary aerodynamic characterization of high-speed vehicles to support mission analysis. *ICAS - International Council of the Aeronautical Sciences*, 2022.

[9] S. Graziani, N. Viola, F. Petrosino, and J. Jäschke. Comparison between simplified approach and cfd & propagation tool for sonic boom estimation. *AIAA Aviation Forum*, 2023.

[10] C. V. Munoz, G. Bonavolontà, C. Lawson, and A. Riaz. Conceptual design of a next generation supersonic airliner for low noise and emissions. *AIAA SciTech*, 2023.

[11] International Civil Aviation Organisation. Annex 16 — environmental protection, volume ii — aircraft engine emissions. *International Standards and Recommended Practices*, 2008.

[12] International Civil Aviation Organisation. Annex 16 — environmental protection, volume i — aircraft noise. *International Standards and Recommended Practices*, 2017.

[13] International Civil Aviation Organisation. Destination green: The next chapter. *Environmental Report: Aviation and Environment*, 2019.

[14] International Civil Aviation Organisation. Default life cycle emissions values for corsia eligible fuels. *Annex 16 — Environmental Protection, Volume IV — Carbon Offsetting and Reduction Scheme for International Aviation*, 2022.

[15] International Civil Aviation Organisation. Methodology for calculating actual life cycle emissions values. *Annex 16 — Environmental Protection, Volume IV — Carbon Offsetting and Reduction Scheme for International Aviation*, 2022.

[16] International Civil Aviation Organisation. Jet aeroplanes emissions database. *Certification Emissions Levels*, 2023.

[17] International Civil Aviation Organisation. Jet aeroplanes noise database. *Certification Noise Levels*, 2023.

[18] N. Pavlenko, S. Y. Searle, and A. Christensen. The cost of supporting alternative jet fuels in the european union. *The International Council on Clean Transportation*, 2019.

[19] M. Prussi, U. Lee, M. Wang, R. Malina, H. Valin, F. Taheripour, C. Velarde, M. D. Staples, L. Lonza, and J. I. Hileman. Corsia: The first internationally adopted approach to calculate life-cycle ghg emissions for aviation fuels. *Renewable and Sustainable Energy Reviews*, 2021.

[20] D.P. Raymer. *Aircraft Design: A Conceptual Approach*. AIAA education series. American Institute of Aeronautics and Astronautics, Incorporated, 2018.

[21] A. W. Robins, S. M. Dollyhigh, F. L. Beissner, K. Geiselhart, G. L. Martin, E. W. Shields, E. E. Swanson, P. G. Coen, and S. J. Morris. Concept development of a mach 3.0 high-speed civil transport. *NTRS - NASA Technical Reports Server*, 1988.

[22] J. Roskam. *Airplane Design*. DAR Corporation, 2018.

[23] M. H. Sadraey. *Aircraft Design: A Systems Engineering Approach*. Aerospace Series. Wiley, 2013.

[24] J. Soone. Sustainable aviation fuels. *European Parliament*, 2020.

[25] E. Torenbeek. *Essentials of Supersonic Commercial Aircraft Conceptual Design*. Aerospace Series. Wiley, 2020.